CrossMark

ORIGINAL PAPER

A model for one-dimensional morphoelasticity and its application to fibroblast-populated collagen lattices

Shakti N. Menon[1,2,3] · Cameron L. Hall[4,5] · Scott W. McCue[2] · D. L. Sean McElwain[2,3]

Abstract The mechanical behaviour of solid biological tissues has long been described using models based on classical continuum mechanics. However, the classical continuum theories of elasticity and viscoelasticity cannot easily capture the continual remodelling and associated structural changes in biological tissues. Furthermore, models drawn from plasticity theory are difficult to apply and interpret in this context, where there is no equivalent of a yield stress or flow rule. In this work, we describe a novel one-dimensional mathematical model of tissue remodelling based on the multiplicative decomposition of the deformation gradient. We express the mechanical effects of remodelling as an evolution equation for the effective strain, a measure of the difference between the current state and a hypothetical mechanically relaxed state of the tissue. This morphoelastic model combines the simplicity and interpretability of classical viscoelastic models with the versatility of plasticity theory. A novel feature of our model is that while most models describe growth as a continuous quantity, here we begin with discrete cells and develop a continuum representation of lattice remodelling based on an appropriate limit of the behaviour of discrete cells. To demonstrate the utility of our approach, we use this framework to capture qualitative aspects of the continual remodelling observed in fibroblast-populated collagen lattices, in particular its contraction and its subsequent sudden re-expansion when remodelling is interrupted.

Keywords Morphoelasticity · Biomechanics · Tissue plasticity · Fibroblast-populated collagen lattices

Mathematics Subject Classification 74L15 · 92C10 · 74D10

✉ Scott W. McCue
scott.mccue@qut.edu.au

1 Present Address: The Institute of Mathematical Sciences, CIT Campus, Taramani, Chennai 600113, India

2 School of Mathematical Sciences, Queensland University of Technology, Brisbane, QLD 4001, Australia

3 Institute of Health and Biomedical Innovation, Queensland University of Technology, Brisbane, QLD 4001, Australia

4 Present Address: Mathematics Applications Consortium with Science and Industry, University of Limerick, Castletroy, Limerick V94 T9PX, Ireland

5 Oxford Centre for Industrial and Applied Mathematics, Mathematical Institute, University of Oxford, 24-29 St Giles', Oxford OX1 3LB, UK

1 Introduction

In this study, we present a one-dimensional mathematical model of biological tissue remodelling, based on the multiplicative decomposition of the deformation gradient. An important feature of our model is that the mechanical effects of remodelling are expressed in terms of an evolution equation for the 'effective strain'—a measure of the difference between the current state and a hypothetical mechanically relaxed state of the tissue. This morphoelastic model combines the simplicity and interpretability of classical viscoelastic models with the versatility of plasticity theory. To demonstrate its utility, we show that this model can quantitatively capture aspects of the mechanical behaviour of fibroblast-populated collagen lattices reported in previous experiments.

As biological tissues deform continuously when subjected to mechanical forces, their physical behaviour is often modelled using classical continuum mechanics (Mur-

Springer

ray 2001). However, unlike classical solids, living tissues may contain cells that can modify the fundamental mechanical properties of their physical environment. There are a number of processes, most notably tissue growth, in which cells cooperatively alter the tissue structure, changing the relationship between stress and deformation (Chen and Hoger 2000). Indeed, many tissues undergo a continual process of internal revision and mechanical restructuring, often referred to as 'remodelling' (Taber 1995), in which physical properties of the material, including anisotropy and stiffness, evolve over time. This active remodelling is thought to be significant in a wide range of biological processes such as embryo development and morphogenesis (see Patwari and Lee (2008) for a recent discussion). In particular, it is well known that fibroblast cells, which are found in the stroma of numerous tissues, actively remodel the surrounding extracellular matrix (ECM) by synthesising and reorganising collagen fibres, and that this remodelling is essential for tissue homeostasis and for wound repair (Grinnell 2003; Majno and Joris 2004). Remodelling also affects the mechanical stresses experienced by cells in a tissue, which can subsequently modify aspects of cell behaviour. For instance, fibroblasts are known to change their morphology (Tamariz and Grinnell 2002; Tomasek et al. 2002; Gabbiani 2003) and phenotype (Tomasek et al. 2002; Amadeu et al. 2003; Gabbiani 2003) in response to external mechanical cues. Most significantly, the mechanical stresses experienced by fibroblasts during the wound healing process stimulate them to differentiate into more contractile forms: proto-myofibroblasts and myofibroblasts (Gabbiani et al. 1972; Tomasek et al. 2002; Desmoulière et al. 2005), which play a major rôle in the subsequent contraction of the wound. The interplay between mechanical stress and active remodelling is hence critically important in wound healing, as excessive contraction is known to lead to pathologies, such as hypertrophic scars and contractures (Roseborough et al. 2004; Enoch and Leaper 2005; Murphy et al. 2011b).

Since the first descriptions of the kinematics of biological growth the 1970s and early 1980s (Taber 1995; Humphrey 2003), several theoretical frameworks have been proposed to capture the dynamics of remodelling. A very significant advance in this direction was made in the mid 1990s, when Rodriguez et al. (1994) and Cook (1995) independently developed a mathematical framework for remodelling that utilises the *multiplicative decomposition of the deformation gradient*—an idea that dates back to the 1950s (Bilby et al. 1957; Kröner 1958, 1959), and which was formalised in the 1960s by Stojanović et al. (1964, 1970) and Lee (1969). In this paper, we use the notation developed by Goriely and coworkers (Goriely and Ben Amar 2007; Goriely et al. 2008; Vandiver and Goriely 2009; Goriely and Moulton 2011),
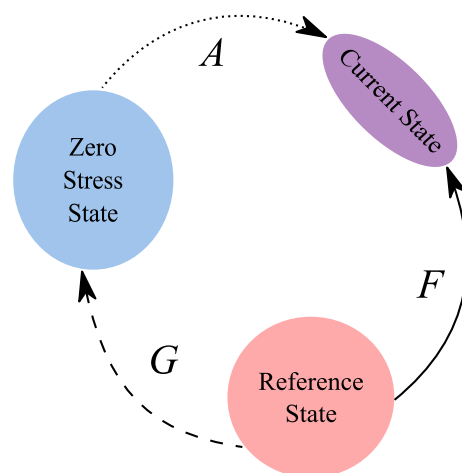

Fig. 1 The relationship between the reference state, the current state and the zero stress state. In our notation, F represents the overall deformation gradient from the reference state to the current state, while the plastic/growth component G represents the deformation from the reference state to the zero stress state and the elastic component A represents the deformation from the zero stress state to the current state

where A and G represent the elastic and plastic/growth parts of the deformation gradient, respectively. The decomposition of the deformation gradient tensor thus yields the expression

$$F = A\,G. \tag{1}$$

The physical interpretation of this decomposition is depicted in Fig. 1: G is the deformation gradient tensor associated with a hypothetical deformation from the fixed reference state to a state where all internal stresses are relieved, while A represents the deformation from this 'zero stress state' to the current state. For a purely elastic material, the fixed reference state will also be the zero stress state, and we find that $G \equiv I$. However, plastic flow or remodelling enables the zero stress state, and hence G, to evolve. A detailed discussion of the fundamental concepts that underlie the multiplicative decomposition of the deformation gradient is presented in 'Appendix 1'.

This approach not only provides a clear and coherent way of understanding growth, but also leads to a natural way of describing 'residual stress'—stress that persists even when all loads are removed. Although Fung (1993) had noted much earlier that some tissues (such as arteries) are structured so that it is impossible for the entire tissue to be free of residual stresses unless cuts are made, limited attempts had been made to describe these stresses mathematically. An alternative paradigm was suggested by Goriely and Ben Amar (2007), who coined the term *morphoelasticity* to describe the combination of elastic and 'plastic' changes that are the result of biological growth and remodelling. Despite some similarities, morphoelasticity is quite distinct from classi-

cal plasticity. For example, morphoelastic remodelling will generally occur throughout a tissue, not just in those regions where a yield stress is exceeded. Moreover, morphoelasticity can involve changes to the total mass of a tissue (in tissue growth, for example) and/or increases in internal energy, while plastic flow is always mass conserving and dissipative. This framework has been recently used to mathematically describe aspects of wound healing, namely wound contraction and scar formation (Yang et al. 2013) and dermal wound closure (Bowden et al. 2016), as well as growth in other biological tissues such as axons (García-Grajales et al. 2016).

While remodelling is important in a wide range of phenomena *in vivo*, surprisingly few *in vitro* experiments have been developed to explicitly study the macroscopic consequences of remodelling. A notable counter-example is the investigation of the contraction of fibroblast-populated collagen lattices (FPCLs)—cultured fibroblasts embedded in (or placed on top of) three-dimensional (3-D) collagen matrices. It has long been known that FPCLs can contract to a small fraction of their initial size within a few days (Bell et al. 1979). This contraction was first observed to be 'permanent' by Grinnell and coworkers (Grinnell and Lamke 1984; Guidry and Grinnell 1985, 1986), who validated this finding by performing several experiments with varying numbers of fibroblast cells that were placed on top of collagen lattices of different initial densities. Most fibroblasts did not invade the lattice and were instead found to spread over its surface while reorganising proximal collagen fibres in the direction of spreading. It was thus proposed that the reorganisation of the lattice away from the cells was chemically mediated by the secretion of cell-binding factors such as fibronectin and proteoglycans (Grinnell and Lamke 1984). It was also observed that the addition of cytochalasin D, which suppresses gel reorganisation by inhibiting cell motility, resulted in a partial re-expansion of the gel (Guidry and Grinnell 1985, 1986). The relative magnitude of the re-expansion was found to be smaller in gels that were contracted by fibroblasts for a greater period of time, which suggested that the collagen gels were first physically reorganised by fibroblasts and then stabilised by the continued presence of these cells.

In this work, we develop a mathematical description of the contraction of FPCLs that incorporates the mechanical effects of remodelling. In Sect. 2, we provide a detailed summary of FPCLs and the different mechanisms by which they can permanently contract. Then, in Sect. 3, we construct an expression for the rate of morphoelastic contraction of an FPCL, based on a plausible microscopic mechanism of cells rearranging the fibres of the lattice. On varying the two free parameters of this simplified model, we quantitatively replicate features of previous experiments on contracting FPCLs. Finally, in Sect. 4 we discuss how our framework is significantly advantageous in comparison with many other

approaches to describing remodelling in biological tissues, and detail possible extensions to our model.

2 Fibroblast-populated collagen lattices

2.1 History and classification

FPCLs were developed by Elsdale and Bard (1972), who used them as a means of investigating fibroblast behaviour in a setting that closely resembles their natural environment. A scanning electron microscope image of a fibroblast embedded in a collagen lattice, taken from Rhee and Grinnell (2007), is shown in Fig. 2. Experiments on such lattices can provide insight into the mechanical interactions between fibroblasts and surrounding collagen fibrils. Since first being developed, these lattices have been used to study the traction forces exerted by fibroblasts in mechanically relaxed (Bell et al. 1979; Bellows et al. 1981; Ehrlich and Rajaratnam 1990) and in mechanically loaded environments (Guidry and Grinnell 1985; Mudera 2000; Hinz et al. 2001). FPCLs have also been used to investigate the effects of various growth factors on fibroblasts (Grinnell et al. 1999; Schreiber et al. 2001) as well as the behaviour of individual fibroblasts as they contract their environment while moving through the ECM (Roy et al. 1997, 1999). Further details on the range of experiments involving FPCLs, and their clinical utility, are provided in the reviews by Grinnell (2003), Dallon and Ehrlich (2008), and Ehrlich and Moyer (2013).

FPCLs are typically classified according to the mechanical set-up that is used to create them. By this reckoning, there
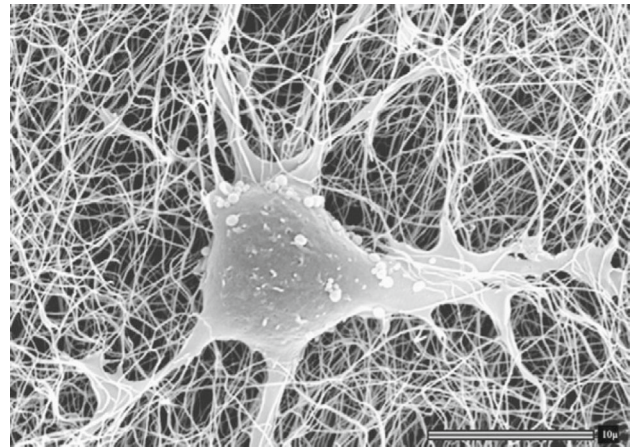

Fig. 2 Scanning electron microscope image of a human fibroblast interacting with 3D collagen matrices. Here, the fibroblast exhibits a dendritic structure, indicating that the environment is unstressed. The scale in the figure represents 10 μm (Reprinted from *Advanced Drug Delivery Reviews* 59(13), Rhee S. and Grinnell F., *Fibroblast mechanics in 3D Collagen matrices*, pp 1299–1305, Copyright (2007) with permission from Elsevier)
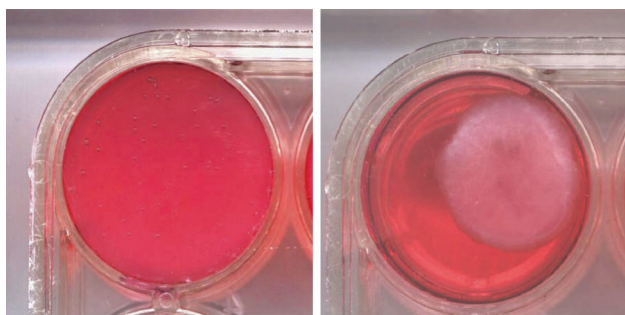
Fig. 3 Contraction of a solidified free-floating FPCL. The *left image* shows the initial configuration of a collagen gel, while the *right image* shows the configuration of the same gel after 48 h (with kind permission from Springer Science+Business Media: *Methods in Molecular Biology: Kidney Research*, Chapter 14. *Cell-Populated Floating Collagen Lattices: An In Vitro Model of Parenchymal Contraction*, 466, 2009, 1–11, Kelynack, K.J., Fig. 14.1)

are three main types of FPCLs: free-floating, attached and stress-relaxed.

Free-floating FPCLs were introduced by Bell et al. (1979) and are prepared by polymerising a collagen gel with fibroblasts. This could be done either in a bacteriological dish, to which the gel adheres poorly, or in a tissue culture dish, in which case the gel has to be detached after a certain time. The image displayed in Fig. 3, taken from Kelynack (2009), shows an example of a free-floating FPCL. In such lattices, the fibroblasts project a dendritic network of extensions and the tension is distributed isotropically (Grinnell et al. 2003; Rhee and Grinnell 2007).

Fibroblasts in free-floating lattices can generate significant traction forces (Grinnell 2000; Majno and Joris 2004), which reorganise the matrix and lead to contraction. While this reorganisation does not orient collagen fibrils in any particular direction, it can still cause these lattices to contract to as little as a tenth of their initial lateral (or vertical) extent (Bell et al. 1979; Steinberg et al. 1980; Grinnell and Lamke 1984; Guidry and Grinnell 1985), even in the absence of protomyofibroblast cells, which can exert greater forces. This contraction gives rise to a mechanically relaxed tissue that resembles dermis, and it has hence been proposed that such lattices can be used to describe the earliest stages of wound healing, before inflammation and tissue stress have activated the differentiation of fibroblasts into myofibroblasts (Grinnell 1994). Such FPCLs are observed to remain disc shaped throughout the contraction process, which involves a reduction in thickness as well as diameter, although the edges of the disc are observed to eventually curl up (Bell et al. 1979).

Attached FPCLs are fibroblast-populated lattices that are polymerised in a tissue culture dish, to which the gel attaches firmly. A consequence of this experimental arrangement is that the lattices decrease in thickness, but not in lateral area (Grinnell and Lamke 1984; Guidry and Grinnell 1985). The

tension in such lattices is distributed anisotropically, while fibroblasts develop an elongated bipolar appearance, orienting themselves along the lines of tension (Bellows et al. 1982; Stopak and Harris 1982; Grinnell 1994; Tamariz and Grinnell 2002). This reorganisation causes collagen fibrils to become oriented in the same plane as the substrate, which in turn gives rise to mechanical loading within the matrix. The contraction of such lattices, which involves a reduction in thickness alone, gives rise to a mechanically stressed tissue resembling granulation tissue, and it has therefore been proposed that such lattices can be used to model the early stage of wound healing when the granulation tissue begins to develop and exert stresses on its environment (Grinnell 1994). The rate and extent of contraction of the lattice are similar to that in experiments where fibroblasts are embedded within such lattices (Grinnell and Lamke 1984; Guidry and Grinnell 1985, 1986). Fibroblasts in such lattices organise a fibronectin matrix and develop prominent actin stress fibres (Farsi and Aubin 1984; Mochitate et al. 1991; Halliday and Tomasek 1995), which indicate that some fibroblasts have differentiated into the protomyofibroblast phenotype. It has also been observed that fibroblasts in restrained matrices develop fibronexus junctions (Tomasek et al. 2002), which allow TGF-β, if present, to further stimulate the differentiation of protomyofibroblasts into the myofibroblast phenotype (Arora et al. 1999; Vaughan et al. 2000).

A *stress-relaxed FPCL* is prepared by polymerising collagen lattice, allowing it to attach to a tissue culture dish for a set period of time and then detaching it (Tomasek et al. 1992). In such lattices, tensile stress develops while the matrix is anchored and these stresses are relieved via a sudden smooth muscle-like contraction when the matrix is released, as the cell extensions collapse and the stress fibres disappear (Mochitate et al. 1991; Tomasek et al. 1992; Lin et al. 1997). It has been proposed that stress-relaxed FPCLs can be used to model scar tissue, or the transition from granulation tissue to replacement dermis in wound healing or in tissue repair (Carlson and Longaker 2004).

As discussed earlier, the contraction of an FPCL results from a fundamental reorganisation of the lattice structure and is hence effectively 'permanent'. We now discuss the mechanisms that have been proposed to explain the contraction of FPCLs.

2.2 Mechanical properties

It is known that the degradation and replacement of collagen fibres is not a significant mechanism of contraction in attached lattices. This was demonstrated experimentally using radiolabelled collagen, where it was found that the concentration of proteins in the gel remains constant during the reorganisation process (Guidry and Grinnell 1985). Indeed, it seems plausible to assume that contraction in all types of

FPCLs is largely a result of the rearrangement of pre-existing collagen fibres by fibroblasts. Even still, the precise mechanism of lattice contraction is thought to vary, depending on the density and mechanical state of the lattice.

The prime mechanism of stressed lattice contraction is believed to be *cell contraction*, which is associated with the protomyofibroblast and myofibroblast phenotypes that are prevalent in such environments (Dallon and Ehrlich 2008). When these cells contract, they pull on the surrounding lattice, causing it to contract with them. It has been suggested that contraction in free-floating lattices of moderate cell density occurs through a *cell traction* mechanism (Dallon and Ehrlich 2008), in which cell locomotion results in the compacting of collagen fibres by bundling thin fibrils (Harris et al. 1980; Ehrlich 2003). As discussed in Dallon and Ehrlich (2008), the contraction of free-floating lattices of high cell density is believed to occur through a *cell elongation and spreading* mechanism, in which fibroblasts pull collagen fibrils towards them, thus compacting the gel.

A salient feature of FPCLs is that they provide a testbed for investigating how the interplay between fibroblasts and the collagen matrix can cause the latter to permanently contract. Under the action of fibroblasts, the density of neighbouring fibrils increases locally and consequently the volume of the collagen lattice decreases (Grinnell 2003). An example of such behaviour, taken from an experiment by Kelynack (2009), is shown in Fig. 3.

The observation that the lattices only re-expand partially crucially indicates that contraction is not simply the elastic response of the collagen lattice to traction forces applied by cells. Unlike other forms of remodelling, such as the hardening of the human eye lens described by Augusteyn (2010), which could be modelled using a time-dependent stress–strain relationship, FPCL contraction involves some form of cell-induced 'plastic' behaviour. That is, the active lattice remodelling by cells causes the unloaded state of the lattice to change over time in a manner analogous to classical plasticity. Hence, a central aim of this paper is to develop a mathematical framework for FPCL contraction that takes into account the evolving unloaded state. Our approach quantitatively captures key features of the contraction process, which would be impossible to achieve with, for example, a Kelvin–Voigt viscoelastic constitutive law. We now briefly outline some of the previous mathematical approaches to modelling the behaviour of FPCLs.

2.3 Modelling FPCL contraction

Most previous models of FPCL contraction have incorporated a viscoelastic framework. The earliest such model was developed by Moon and Tranquillo (1993), who adapted the Tranquillo and Murray (1992) model of dermal wound healing to describe the contraction of a collagen micro-sphere. This model could not, however, account for the permanence of matrix contraction. An alternative framework, which addresses this issue, but which is only valid for small displacement gradients, was developed by Barocas et al. (1995) who replaced the Kelvin–Voigt constitutive law in the Moon–Tranquillo model with a Maxwell constitutive law. In contrast, Ferrenq et al. (1997) retained the linear Kelvin–Voigt constitutive law, but restricted their focus to situations in which the displacement gradient is small and linear theory is valid. A different approach, that used the theory of mixtures to describe the interaction between the fibrous lattice and the permeating fluid medium, was the biphasic model of collagen lattice contraction developed by Barocas and coworkers (Barocas and Tranquillo 1994, 1997). This model takes into account several important effects, including the partial expansion of collagen lattices after cell traction stresses are removed. Subsequently, Barocas and coworkers have used similar approaches to describe several experiments on collagen lattices (see, for example, Knapp et al. (1999); Schreiber et al. (2003); Chandran and Barocas (2004)), using models that include fibroblast traction as an additive contribution to the total stress. Recent approaches to modelling FPCL contraction include models by Marquez, Zahalak and coworkers (for instance (Zahalak et al. 2000; Pryse et al. 2003; Marquez et al. 2005)), who considered individual cells and used Eshelby's solution to describe the local strain fields and Green et al. (2013), who considered spherical-symmetric collagen lattices and treated the gel as a compressible Stokes fluid.

While these models have significantly advanced the understanding of this process, there have not yet been any models that explicitly take into account the continual mechanical restructuring of such lattices. In the next section, we introduce a morphoelastic model, based on the concept of an 'effective strain' that can be used to capture the remodelling of FPCLs.

3 A morphoelastic model for the contraction of fibroblast-populated collagen lattices

In this section, we develop a mechanical model that can be used to describe the contraction of a collagen lattice by fibroblasts. As described in standard continuum mechanics texts (for example Gonzalez and Stuart (2008)), it is common to work in either a 'Lagrangian' (or 'material') coordinate system, in which each particle is labelled according to its position in the initial configuration of the body, or in an 'Eulerian' (or 'spatial') coordinate system, in which each particle is labelled according to its current position. Holding the Lagrangian coordinate constant corresponds to observing a single particle, while holding the Eulerian coordinate constant corresponds to observing a single point in space.

As we discuss in Sect. 3.2, it is often appropriate to treat contracting FPCLs as 1-D bodies. Indeed, Ferrenq et al. (1997) constructed a model of FPCL contraction in 1-D Cartesian coordinates and various authors have assumed radial symmetry to develop 1-D descriptions of FPCL contraction (Moon and Tranquillo 1993; Ramtani et al. 2002; Ramtani 2004). We hence derive a one-dimensional model, based on the following equation (derived explicitly in 'Appendix 1') that is appropriate for describing the mechanical behaviour of morphoelastic solids with small effective strain

$$\frac{\partial e^E}{\partial t} + \frac{\partial}{\partial x}\left(e^E v\right) = \frac{\partial v}{\partial x} - g(x, t), \tag{2}$$

where e^E is the Eulerian strain, v is the velocity of a point in the material, and $g(x, t)$ describes the rate of growth. As discussed in more detail in 'Appendix 1', Eulerian strain is taken here to be the *effective* Eulerian strain, a local, dimensionless measure of the difference between the current state and the zero stress state, while the rate of growth is a measure of the rate at which the zero stress state becomes larger over time. In Sect. 3.1, we take advantage of the simplifications that can be made to Eq. (2) when the deformation of the lattice might be large, but the difference between the current state and the stress-free state is always small. In particular, we introduce a form for the growth function, $g(x, t)$, based on a plausible mechanism for the contraction of the lattice by fibroblasts. This ultimately leads to a full model of FPCL contraction, which we present in Sect. 3.2.

3.1 A cell-based contraction model

In the experiments performed by Guidry and Grinnell (1985), lattices were contracted by fibroblasts and then allowed to undergo a partial re-expansion after reorganisation is inhibited. This re-expansion was faster than the contraction process, but far from instantaneous, indicating that the timescale associated with the viscous relaxation of collagen lattices should not be ignored. It is hence preferable for us to use a Kelvin–Voigt viscoelastic constitutive law to relate stress and effective strain instead of the purely elastic law, namely $\sigma = E e^E$, described in Appendix section 'Strain evolution'.

Additionally, the large deformations associated with lattice contraction may cause significant changes to the elastic properties of the collagen: we expect the collagen to become stiffer as it becomes denser. Following Ramtani et al. (2002) and Ramtani (2004), we therefore propose that the elastic modulus of the collagen should be a function of collagen density. Incorporating viscoelasticity and the changing elastic modulus (but ignoring the activity of cells), this means

that an appropriate constitutive law for a collagen lattice will take the form

$$\sigma = \mathcal{E}(\rho)\, e^E + \mu\, \frac{\partial v}{\partial x}, \tag{3}$$

where $\mathcal{E}(\rho)$ is the elastic modulus, ρ is the collagen density, and μ is the collagen viscosity.

Next, we develop an expression for $g(x, t)$ that captures how cells actively rearrange the fibres of the collagen lattice by applying traction—a microscopic mechanism that causes a modification in size of the zero stress state. Our approach is to imagine the collagen lattice as a 1-D body containing evenly spaced fibroblasts, each of which effectively acts as a force dipole by pulling on the collagen lying on either side of it and compressing the collagen directly under it. We assume that each fibroblast rearranges the collagen directly under itself, thus evolving the lattice to a permanently compressed state. Thus, $g(x, t)$ will be negative and directly proportional to the compressive strain in the lattice under the cells. Specifically, we assume that $g(x, t)$ is proportional to the amount that the strain in the region covered by the cells e_{cells} exceeds (*i.e.* is more negative than) a critical level of contraction, $-\hat{e}_{\text{crit}}$.

It has been observed that even though fibroblasts lead to substantial deformation of the environment, large strains are confined to regions around each cell (Sander 2013), which results in heterogeneity in collagen density. Hence, to realistically describe the interplay of cells with their environment, one would need to assume that gel compaction is not spatially homogeneous, along the lines of the models by Evans and Barocas (2009) or Stevenson et al. (2010). This approach would introduce a range of complications that do not appear to be physically relevant to FPCLs; as noted in Grinnell and Lamke (1984), apparently homogeneous compaction of a gel is observed even when cells are cultured purely on the gel surface.

For simplicity and brevity, in the analysis that follows we assume that the FPCL consists of a periodic array of identical units, each of which contains a single cell at its centre (see Fig. 4) and hence that the fibroblast density is spatially constant. We assume that the traction forces applied by cells create regions of the lattice (under the cells) that are more
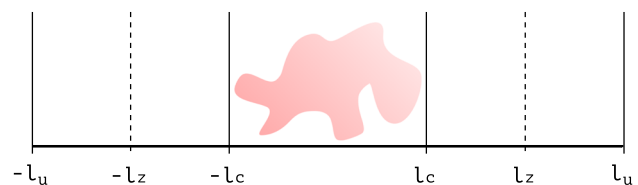

Fig. 4 A single cell within a periodic unit. The cell extends from $-l_c$ to l_c, and the unit extends from $-l_u$ to l_u. The entire region has a uniform zero stress state, and the length of the unit at zero stress is l_z

compressed than other regions of the lattice (outside the cells). However, we also assume that the zero stress state remains homogeneous in space even as it evolves over time. This modelling choice is made in order to account for some effects of cell mobility. We assume that cells make local changes to the zero stress state and then move nearby and repeat this process. The overall effect of this will be for the changes to the zero stress state to be homogenised through space.

Using our assumption of a periodic array of cells, we construct a local coordinate system in which a given unit extends from $-l_u$ to l_u and the cell extends from $-l_c$ to l_c. Thus, the cell density, n, is proportional to l_c/l_u. We also assume that the zero stress state is uniform across the unit and that if the unit was stress-free throughout, it would extend from $-l_z$ to l_z. Hence, the average effective strain throughout the unit is

$$e_{\text{avg}} = \frac{l_u - l_z}{l_u}. \tag{4}$$

Note that a further advantage of the assumption of uniform cell density across the array is that this expression for strain will be equivalent to that measured in a representative volume element containing many cells. We shall therefore use this measure of strain in our macroscopic model.

As the cell in each unit pulls the lattice in towards itself, the collagen under the cell will be under less tension (or more compression) than that over the rest of the unit. More formally, a cell in a given unit can be treated as a pair of body forces, both of magnitude τ_c; at $-l_c$ the cell pulls the collagen lattice to the right, while at l_c the cell pulls the lattice to the left. Neglecting inertial terms, the momentum balance equation within a single unit is then

$$\frac{\partial \sigma_u}{\partial x} = \tau_c \left(\delta(x - l_c) - \delta(x + l_c) \right),$$

where σ_u is the local stress and δ is the Dirac delta function. Integrating this equation with periodic boundary conditions, we find that the stress within the unit is

$$\sigma_u = \begin{cases} \sigma_{\text{out}}, & l_c < |x| < l_u, \\ \sigma_{\text{out}} - \tau_c, & |x| < l_c. \end{cases}$$

where σ_{out} represents the stress in the regions outside the cells, which we assume to be governed by the constitutive law (3), so that

$$\sigma_{\text{out}} = \mathcal{E}(\rho) \, e_{\text{out}} + \mu \frac{\partial v}{\partial x}. \tag{5}$$

Since each cell must apply a balanced pair of body forces to the lattice, it follows that either the boundary of the lattice occurs in a region where $\sigma = \sigma_{\text{out}}$, or there is an additional surface traction term that accounts for the effects of the end

of the cell. In either case, we find that it is most convenient to express macroscopic boundary conditions in terms of σ_{out}: a free-floating lattice will have $\sigma_{\text{out}} = 0$ on the boundary, while a spring connected to the boundary (as in, for example, Marenzana et al. (2006)) should be expressed as a relationship between σ_{out} and the displacement at the boundary.

From the definition of strain above, we can express τ_c as

$$\tau_c = \sigma_{\text{out}} - \sigma_{\text{cells}}, \tag{6}$$

where σ_{cells} is the stress in the region covered by the cell. Assuming that viscous stresses are uniform (or negligible) between l_c and $-l_c$, and using a constitutive law for σ_{cells}, we obtain the expression

$$e_{\text{cells}} = \frac{\sigma_{\text{out}} - \tau_c}{\mathcal{E}(\rho)}.$$

As mentioned earlier, we assume that the growth rate $g(x, t)$ is dependent on the physical contraction experienced by the lattice directly under the cells and is proportional to $-(e_{\text{cells}} - \hat{e}_{\text{crit}})$. Moreover, the rate of contraction is proportional to the cell density, n, as this is representative of the proportion of the lattice that is accessible to the fibroblasts. Thus, we obtain the following constitutive law for $g(x, t)$:

$$g(x, t) = -\theta n \left(-\frac{\sigma_{\text{out}} - \tau_c}{\mathcal{E}(\rho)} - \hat{e}_{\text{crit}} \right)^+, \tag{7}$$

where θ is a constant of proportionality with dimensions of cell density^{-1} time^{-1} and the positive part operator $(X)^+ = X$ for any positive X and is zero otherwise. As the condition

$$\hat{e}_{\text{crit}} < -\frac{\sigma_{\text{out}} - \tau_c}{\mathcal{E}(\rho)}$$

is always satisfied in most practical situations, we neglect the positive part operator in (7) for the rest of our analysis.

Next, we note that since the zero stress state is uniform throughout the unit,

$$l_u - l_z = e_{\text{cells}} \, l_c + e_{\text{out}} (l_u - l_c). \tag{8}$$

Combining this with (4) yields the expression

$$e_{\text{avg}} = e_{\text{out}} + \frac{l_c}{l_u} \left(e_{\text{cells}} - e_{\text{out}} \right).$$

Using (6), and defining σ_c as rescaling of τ_c so that $n \, \sigma_c = l_c/l_u \, \tau_c$, we obtain

$$e_{\text{out}} = e_{\text{avg}} + \frac{n \, \sigma_c}{\mathcal{E}(\rho)}.$$

Substituting into (5) gives us our constitutive relationship between stress and strain:

$$\sigma_{\text{out}} = \mathcal{E}(\rho)\, e_{\text{avg}} + \mu\, \frac{\partial v}{\partial x} + n\, \sigma_c.$$

Note that the $n\,\sigma_c$ term is analogous to the cell traction stress term found in other models of lattice contraction and dermal wound healing (Tranquillo and Murray 1992; Moon and Tranquillo 1993; Tracqui et al. 1995; Ferrenq et al. 1997). Indeed, by making σ_c a function of the lattice density and/or cell density (to incorporate the effects of crowding on traction stress, for example), we can recover identical expressions to those used in these earlier papers. However, our approach differs in that traction stress emerges naturally from the assumption that cells apply body forces to the collagen lattice, rather than by requiring that this stress term be incorporated into the constitutive law. Nevertheless, the consistency between these two treatments of cell traction gives us further confidence that both approaches are valid and useful.

Dropping the subscripts on e_{avg} and σ_{out}, we obtain the following set of equations to describe the mechanical behaviour of a contracting viscoelastic lattice:

$$\frac{\partial e}{\partial t} + \frac{\partial}{\partial x}\,(e\,v) = \frac{\partial v}{\partial x} + \theta\, n \left(-\frac{\sigma - n_l\,\sigma_c}{\mathcal{E}(\rho)} - \hat{e}_{\text{crit}} \right), \quad (9a)$$

$$\sigma = \mathcal{E}(\rho)\, e + \mu\, \frac{\partial v}{\partial x} + n\, \sigma_c, \quad (9b)$$

$$\frac{\partial \sigma}{\partial x} = 0, \quad (9c)$$

where $n_l = n\, l_u / l_c$ is the constant of proportionality that relates the cell density, n, to the cell length per unit length, l_c / l_u.

A full description of the mechanics of a contracting lattice will also require an initial condition on e and two boundary conditions, either on σ or v, that specify whether the ends of the lattice are tethered or stress-free. We now combine (9) with some assumptions about fibroblast motion and interactions in FPCLs to construct a full morphoelastic model of FPCL contraction.

3.2 The morphoelastic model of FPCL contraction

In the following, we assume that the contraction of the lattice is due to the rearrangement of collagen fibrils by fibroblasts alone, with the expectation that the results obtained using this assumption will be quantitatively similar to those obtained using a model that takes into account the rôle of protomyofibroblasts. Additionally, we assume that TGF-β is not present in the collagen lattice. As protomyofibroblasts require the presence of TGF-β to differentiate into myofibroblasts (Tomasek et al. 2002), we hence do not consider the activity of the latter. Furthermore, while it has been observed that fibroblasts in free-floating lattices become quiescent (Rosenfeldt and Grinnell 2000) and a small fraction of these cells undergo apoptosis (cell death) (Fluck et al. 1998; Grinnell et al. 1999), we shall neglect these processes in our model.

Experimental data for the contraction of FPCLs are typically obtained by measuring the changing diameter (in the case of free-floating FPCLs) or thickness (in the case of attached FPCLs) of the lattice. The behaviour of such lattices can hence be modelled by considering one spatial dimension that represents either the radius or thickness of the lattice depending on the type of FPCL being considered. It should be noted that the mechanical model presented in 'Appendix 1' assumes a single Cartesian spatial dimension and cannot be easily modified to obtain equations for the mechanics of radially symmetric lattice contraction. As a result, our model is best suited to attached, rather than free-floating, FPCLs. Nevertheless, as seen later in this section, our model is equally successful at fitting data obtained from both these lattice types.

Following the conventions used in Appendix section 'The multiplicative decomposition of the deformation gradient', we use $x(X, t)$ to represent the position at time t of a particle initially located at X and $X(x, t)$ to represent the initial position of a particle at position x at time t. Since the lattice changes in size over time, the domain of interest can be expressed as $0 \leq x \leq l(t)$ or, equivalently, $0 \leq X \leq l_0$, where $l_0 = l(0)$. As illustrated in Fig. 5, the point $x = 0$ is taken to represent either the centre of a floating lattice or the fixed tethering point of an attached lattice. In either case, this point is fixed and we hence find that $x(0, t) = X(0, t) = 0$.

We next define the Eulerian displacement, $u(x, t) = x - X(x, t)$, and the Eulerian displacement gradient, $w(x, t) = \partial u / \partial x$. Following the definitions of x and X, it follows that $u(x, 0) = w(x, 0) = 0$. Moreover, the fact that the centre or tethering point is fixed implies that $u(0, t) = 0$. Another important kinematic variable is the velocity, which is defined as

$$v(x, t) = \frac{\mathrm{D}u}{\mathrm{D}t} = \frac{\partial u}{\partial t} + v\, \frac{\partial u}{\partial x}, \quad (10)$$

with $v(0, t) = 0$ at the fixed centre/tethering point.

Next, we introduce expressions for the densities of the ECM, $\rho(x, t)$, and the fibroblast cells, $n(x, t)$. Since Guidry and Grinnell (1985) observed that collagen synthesis and degradation are insignificant in FPCLs, we propose that contraction proceeds only by rearrangement of the collagen lattice. In other words, we assume that the net creation of each species is zero during the timescale of the experiment. Furthermore, for this study, we assume that there is no migration of fibroblasts. As both species are subjected to passive advection, this assumption allows us to use simple continu-
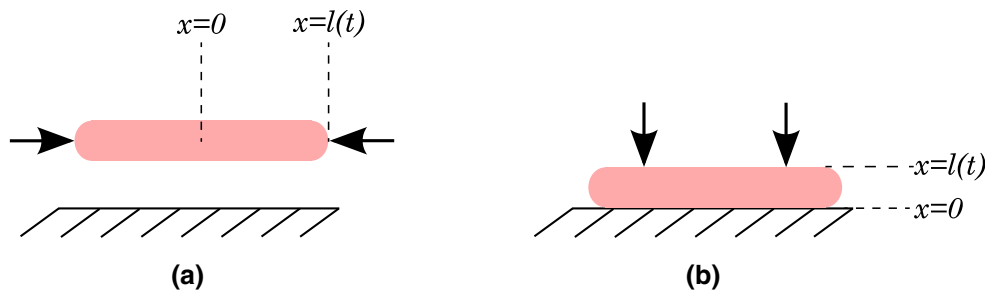
Fig. 5 Sketch of the different situations that can be described using our morphoelastic model. Here the *dashed lines* represent the substrate, and the *arrows* represent the directions of contraction of the collagen lattice (*pink*). **a** In the case of a free-floating FPCL, we have symmetry about $x = 0$. **b** In the case of an attached FPCL, $x = 0$ represents the base of the lattice and $x = l(t)$ is the contracting edge. This situation can be thought of as the case of a lattice with a spring of infinite stiffness attached at $x = 0$

ity equations for each of the species, which can be solved explicitly (Clement 1978) to give

$$n(x, t) = n_0 (1 - w(x, t)), \tag{11}$$
$$\rho(x, t) = \rho_0 (1 - w(x, t)), \tag{12}$$

where n_0 and ρ_0 are the (spatially uniform) initial densities of fibroblast cells and the ECM, respectively.

We assume that the lattice is initially relaxed ($e(x, 0) = 0$) and that lattice stiffness increases with density, according to the simple linear relationship

$$\mathcal{E}(\rho) = \mathcal{E}_0 + k \frac{\rho - \rho_0}{\rho_0},$$

where $\mathcal{E}_0$ is the elastic modulus when $\rho = \rho_0$ and k is a positive constant. It should be noted that other forms have been proposed to describe the dependence of the elastic modulus on density. For example, Ramtani and coworkers describe this relationship as a power law (Ramtani et al. 2002; Ramtani 2004). In the absence of further data, however, we use a simple, linear law.

The case of a free-floating FPCL (Fig. 5a) or an attached FPCL (Fig. 5b) can be described by using the stress-free boundary condition

$$\sigma(l(t), t) = 0, \tag{13}$$

and the displacement at $x = l(t)$ can be obtained by noting that

$$\int_0^{l(t)} w(\xi, t) \mathrm{d}\xi = u(l(t), t) = l(t) - l_0.$$

As we shall see, $w(x, t)$ is spatially homogeneous in the problem that we analyse. In this situation, it follows that

$$l(t) = \frac{l_0}{1 - w}. \tag{14}$$

Taking the spatial derivative of (10) and rearranging, we obtain the following evolution equation for $w(x, t)$:

$$\frac{\partial w}{\partial t} + \frac{\partial}{\partial x} (w\, v) = \frac{\partial v}{\partial x}. \tag{15}$$

In conjunction with the equations for the evolution of the effective strain (9a), the constitutive law for the total stress (9b) and the force balance Eqs. (9c), (11)–(15) comprise an Eulerian model for the contraction of collagen by fibroblasts. This system can be non-dimensionalised by introducing the dimensionless variables

$$x^* = \frac{x}{l_0}, \quad l^* = \frac{l}{l_0}, \quad t^* = \frac{t}{h}, \quad v^* = \frac{v\,h}{l_0}, \quad w^* = w,$$

$$e^* = e, \quad n^* = \frac{n}{n_0}, \quad \rho^* = \frac{\rho}{\rho_0}, \quad \sigma^* = \frac{\sigma}{\mathcal{E}_0}, \quad \mathcal{E}^* = \frac{\mathcal{E}}{\mathcal{E}_0},$$

and the dimensionless constants

$$\bar{\mu} = \frac{\mu}{\mathcal{E}_0\, h}, \quad \bar{k} = \frac{k}{\mathcal{E}_0}, \quad \bar{\tau} = \frac{\sigma_c\, n_0}{\mathcal{E}_0},$$

$$\bar{\theta} = h\, \theta\, n_l, \quad \bar{e}_{\mathrm{crit}} = \frac{\hat{e}_{\mathrm{crit}}\, n_0}{n_l}, \tag{16}$$

where, for ease of comparison with experiment (see later), we choose $h = 1$ h.

3.3 Lagrangian description of the model

As this Eulerian model has a moving boundary at $x = l(t)$, we now adopt a Lagrangian coordinate system to obtain a model for a system in which the right-hand boundary is fixed. Conveniently, we find that transforming our equations to Lagrangian variables is equivalent to converting to characteristic variables: we ultimately obtain a system where the only differentiation is with respect to time. In the derivation that follows, it is important to distinguish between partial time derivatives with the Eulerian spatial coordinate held fixed

and partial time derivatives with the Lagrangian spatial coordinate X held fixed. Hence, we introduce the 'Lagrangian time variable', T, and we transform the entire problem from (x, t) coordinates to (X, T) coordinates.

Firstly, we introduce Lagrangian displacement U and Lagrangian velocity V, which are defined as

$$U(X, T) = x(X, T) - X, \quad V(X, T) = \frac{\partial U}{\partial T}.$$

These are both identical to $u(x, t)$ and $v(x, t)$ with just a transformation of the independent variables (see Appendix section 'Strain evolution' for details). Now, we define the Lagrangian displacement gradient, $W(X, T) = \partial U / \partial X$, which is different from w since differentiation with respect to x is different from that with respect to X. As described in 'Appendix 2', however, the definitions of W and V lead to the identities

$$\frac{\partial}{\partial x} \equiv \frac{1}{1 + W} \frac{\partial}{\partial X}, \tag{17}$$

$$\frac{\partial}{\partial t} \equiv \frac{\partial}{\partial T} - \frac{V}{1 + W} \frac{\partial}{\partial X}, \tag{18}$$

and hence $w = W/(1 + W)$. Based on these identities, it follows that

$$\frac{\partial \phi}{\partial t} + \frac{\partial}{\partial x}(\phi v) = \frac{1}{1 + W} \frac{\partial \Phi}{\partial T}, \tag{19}$$

where $\Phi = \phi(1 + W)$ and where ϕ is a general scalar quantity. This motivates the introduction of Lagrangian variables $N = n(1 + W)$, $R = \rho(1 + W)$, $S = \sigma(1 + W)$ and $E = e(1 + W)$, so that all of the advective time derivatives simply become partial time derivatives. From (11) and (12), we obtain the following exact expressions for the scaled densities N and R in the 'normal' contracting situation

$$N(X, T) \equiv 1, \qquad R(X, T) \equiv 1,$$

Note that the situation in which lattice reorganisation is inhibited by the addition of cytochalasin D at some time, T_{inh}, can be described by taking

$$N(X, T) = \begin{cases} 1, & T \leq T_{\text{inh}}, \\ 0, & T > T_{\text{inh}}. \end{cases} \tag{20}$$

From (15), (9a), (9b) and (9c), we obtain the equations

$$\frac{\partial W}{\partial T} = \frac{\partial V}{\partial X},$$

$$\frac{\partial E}{\partial T} = \frac{\partial V}{\partial X} + N \bar{\theta} \left(\frac{\frac{n_0}{n_l} \frac{S}{1+W} - \bar{\tau}}{\mathscr{E}(W)} - \bar{e}_{\text{crit}} \right),$$

$$S(X, T) = \mathscr{E}(W) E + \bar{\mu} \frac{\partial V}{\partial X} + \bar{\tau} N,$$

$$\frac{\partial S}{\partial X} = 0,$$

where $\mathscr{E}(W)$ is

$$\mathscr{E}(W) = 1 - \bar{k} + \frac{\bar{k}}{1 + W}. \tag{21}$$

Using the stress-free boundary condition (13), it follows that

$$S(X, T) \equiv 0.$$

As W is independent of X, it follows that w is independent of x and hence (14) is valid. Moreover, the fact that W and E are both independent of X means that we can rewrite our system of PDEs as a pair of coupled ODEs for the displacement gradient and strain:

$$\frac{dW}{dT} = -\frac{1}{\bar{\mu}} \left(\mathscr{E}(W) E + \bar{\tau} N \right), \tag{22}$$

$$\frac{dE}{dT} = \frac{dW}{dT} + N \bar{\theta} \left(\frac{\bar{\tau}}{\mathscr{E}(W)} - \bar{e}_{\text{crit}} \right). \tag{23}$$

Although this model has five dimensionless free parameters: $\bar{\mu}$, $\bar{k}$, $\bar{\tau}$, $\bar{e}_{\text{crit}}$ and $\bar{\theta}$, as we show in the next section, we can fix three of these parameters using heuristic arguments, leaving us with a two-component model with two free parameters. Finally, on non-dimensionalising (14) and converting to Lagrangian variables, we find

$$l(t) = 1 + W(T). \tag{24}$$

Thus, our transformed ODE model gives easy access to the evolving length of the lattice, which is the physical variable most easily observed in experiments.

3.4 Comparison with Experimental Data

In the following, we numerically integrate the system (22)–(23) and compare the results with previously obtained data. In particular, we consider the experiments of Bell et al. (1979), Talas et al. (1997) and Feng et al. (2003), which used free-floating FPCLs, as well of Guidry and Grinnell (1985), which was performed using an attached FPCL and in which lattice reorganisation was halted at various times. We first estimate values for the parameters $\mathscr{E}_0$, F_{cell} and σ_0, which we then use to fix the parameters $\bar{\mu}$, $\bar{\tau}$ and $\bar{e}_{\text{crit}}$ for each case (values listed in Table 1).

The initial stiffness of a collagen gel $\mathscr{E}_0$ was measured by Knapp et al. (1997, 1999) to be 1.185 kPa. However, the precise value of this quantity has been found to vary widely, depending on the extent of cross-linking (Discher et al. 2005). As the initial stiffness of the gel was not measured in any of the experiments under consideration, we assume

Table 1 Summary of the experimental values for the number of fibroblast cells in the collagen gel and the initial gel diameter, as well as the estimated values of the initial cell traction stress σ_0 and the parameters $\bar{\mu}$, $\bar{\tau}$ and $\bar{e}_{\text{crit}}$, assuming $\mathcal{E}_0 = 1000$ Pa and $F_{\text{cell}} = 500$ nN/cell

Experiment	C (cells)	d (cm)	σ_0 (Pa)	$\bar{\mu}$	$\bar{\tau}$	$\bar{e}_{\text{crit}} (\times 10^{-3})$
Bell et al. (1979)	7.5×10^6	5.3	1700	2.78	1.699	16.99
Talas et al. (1997)	2.5×10^5	2.18	334.9	2.78	0.3349	3.35
Feng et al. (2003)	2.5×10^6	10	159.2	2.78	0.1592	1.59
Guidry and Grinnell (1985)	1.0×10^5	1.2	442.1	2.78	0.4421	4.42

The remaining model parameters $\bar{\theta}$ and $\bar{k}$ are optimised to fit the model to each set of experimental data (see Table 2)

for the purposes of our simulations that the gel used in each case was a lightly cross-linked collagen lattice, and use the approximate value of the stiffness of such lattices (Discher et al. 2005), namely $\mathcal{E}_0 = 1$ kPa.

Next we note that the total cell traction force will be a product of the applied contraction force per cell F_{cell} and the number of cells in the lattice, C. On dividing this quantity by the cross-sectional area of the lattice, A, we obtain an expression for initial cell traction stress:

$$\sigma_0 = \frac{F_{\text{cell}} C}{A}. \tag{25}$$

The values of C and the initial lattice diameter d (from which we can calculate A) for each of the four experiments are listed in Table 1. Although the value of F_{cell} was not measured in any of the four experiments, there have been several other experiments in which the contraction forces exerted by the cells have been determined using cell-populated lattices attached to force monitors, and a wide range of values of F_{cell} has been reported, ranging from 0.1nN/cell (Eastwood et al. 1996) to 1000 nN/cell (Wakatsuki et al. 2000). Here, we will use the result from Kolodney and Wysolmerski (1992), $F_{\text{cell}} = 500$ nN/cell, which was obtained using fibroblast-populated matrices similar to those used in the experiments by Bell et al. (1979), Guidry and Grinnell (1985), Talas et al. (1997) and Feng et al. (2003).

Now, we note that Eq. (9b) implies that the initial cell traction stress can also be expressed as

$$\sigma_0 = \sigma_c n_0.$$

Rearranging the equation for $\bar{\tau}$ in (16) and using (25) with this alternative expression for σ_0, we find that

$$\bar{\tau} = \frac{F_{\text{cell}} C}{\mathcal{E}_0 A}. \tag{26}$$

Thus, the value of $\bar{\tau}$ can be estimated for each experiment, given the values of C and A.

We next note from (16) that the viscosity of the lattice is given by

$$\mu = \bar{\mu} \, \mathcal{E}_0 \, h. \tag{27}$$

For the purpose of our simulations, we assume that $\mu = 1.0 \times 10^7$ Pa s, a value in agreement with Knapp et al. (1997) who measured the shear viscosity of a collagen gel to be 1.24×10^7 Pa s. As we assume that the initial gel stiffness is $\mathcal{E}_0 = 1$ kPa, we hence set $\bar{\mu} = 2.78$ for all experiments.

Finally, we note that although $\bar{e}_{\text{crit}}$ is difficult to determine experimentally, it can be observed from (16) that it is related to the cell density. Hence, we make the heuristic assumption $\bar{e}_{\text{crit}} = C/(C_f A)$, where C_f represents the characteristic number of fibroblasts in an FPCL. In the following, we choose $C_f = 2 \times 10^6$, which is a reasonable estimate that lies within the range of values of C for the experiments considered here. It is interesting to note that the above assumptions yield a simple relationship $\bar{e}_{\text{crit}} = 10^{-3} \, \bar{\tau}$.

The remaining parameters $\bar{\theta}$ and $\bar{k}$ are difficult to estimate from experiments. In particular, $\bar{\theta}$ arises from the constitutive law for $g(x, t)$ and there are no constraints on its value. Hence, in the following we obtain and use 'best-fit' values of $\bar{\theta}$. Moreover, we note the power law exponent for the relationship between elastic modulus and density used Ramtani and coworkers used (Ramtani et al. 2002; Ramtani 2004) is, to a first order approximation, identical to $\bar{k}$. As this exponent was taken to be a free parameter in these previous approaches, we obtain and use best-fit values of $\bar{k}$.

We now qualitatively describe the behaviour of the FPCL in each of the four experiments under consideration by using the values displayed in Table 1 and varying the free parameters $\bar{\theta}$ and $\bar{k}$ using the MATLAB subroutine *fminsearch*, such that we minimise the difference between the experimental values for the fraction of the original length (diameter or thickness) and the values of $l(t)$, given by (24) at the corresponding measurement times. Specifically, we find the values of $\bar{\theta}$ and $\bar{k}$ that yield the lowest values of the quantity χ^2, defined as:

$$\chi^2 = \sum_i \frac{(\mathscr{O}_i - \mathscr{E}_i)^2}{\mathscr{E}_i}, \tag{28}$$

Table 2 Values of the model parameters $\bar{\theta}$ and $\bar{k}$, obtained from the best fit of the results of the simulations to four different sets of experimental data

Experiment	$\bar{\theta}$	$\bar{k}$	$\chi^2(\bar{\theta}, \bar{k})$	$\chi^2(\bar{\theta}, \bar{k}^-)$	$\chi^2(\bar{\theta}, \bar{k}^+)$	$\chi^2(\bar{\theta}^-, \bar{k})$	$\chi^2(\bar{\theta}^+, \bar{k})$
Bell et al. (1979)	0.89	106.62	0.0147	0.0313	0.0298	0.0244	0.0218
Talas et al. (1997)	5.10	1294.92	0.0037	0.0071	0.0063	0.0045	0.0044
Feng et al. (2003)	16.14	183.85	0.0337	0.0446	0.0434	0.0363	0.0356
Guidry and Grinnell (1985)	0.33	2.97	0.0590	0.0704	0.0685	0.0921	0.0890

Goodness of fit tests are performed by comparing simulations performed using these parameter values with the corresponding experimental data, and the resulting χ^2 values for each case are displayed. In addition, we display χ^2 values for the cases where one of $\bar{\theta}$ and $\bar{k}$ is scaled by factors of $\pm 10\%$ (indicated by a corresponding superscript $\pm$), to characterise the robustness of the individual fits
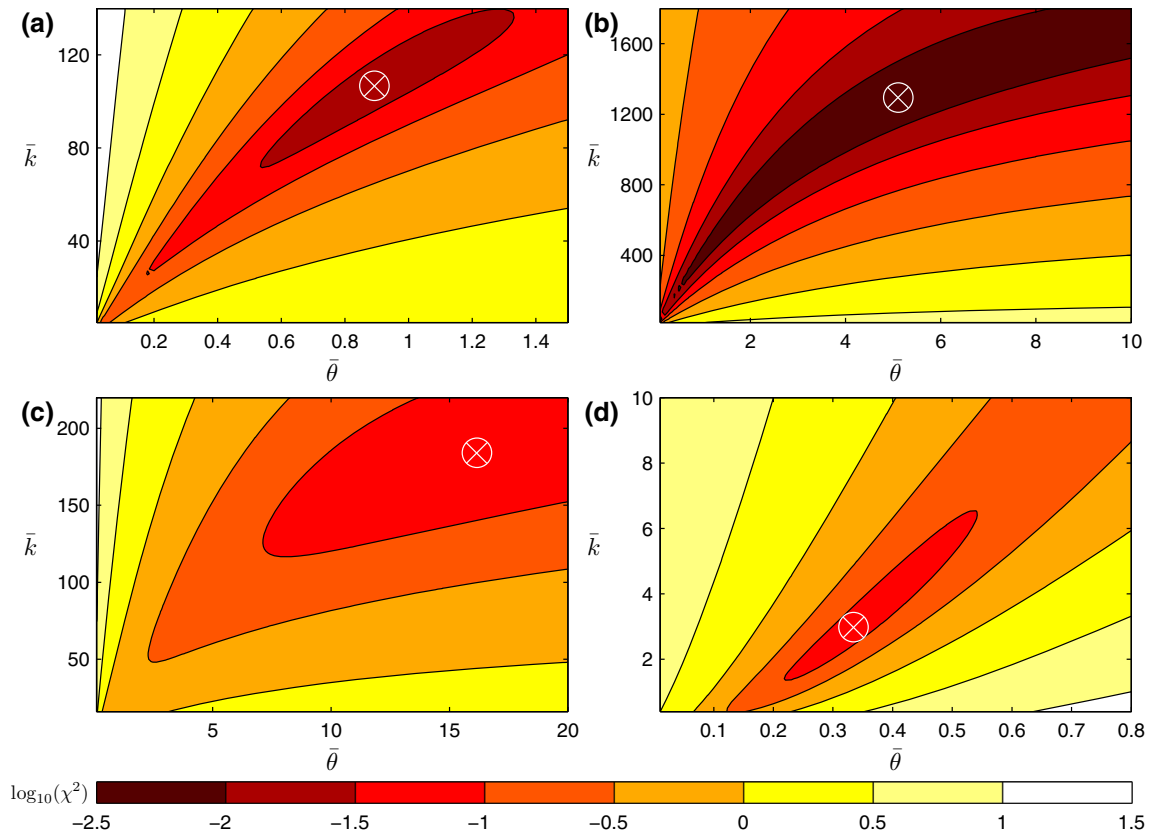
Fig. 6 Contour plots displaying the dependence of the goodness of fit on the free parameters of the model, $\bar{\theta}$ and $\bar{k}$. To capture the variation of the goodness of fit over the parameter space, we display the logarithm (base 10) of $\chi^2(\bar{\theta}, \bar{k})$. The latter quantity is calculated by comparing results obtained by simulating the model for a given value of $\bar{\theta}$ and $\bar{k}$ with experimental data, using Eq. (28). Four experimental datasets are considered, namely **a** data for lattice diameter from Bell et al. (1979), **b** data for lattice diameter from Talas et al. (1997), **c** data for lattice diameter from Feng et al. (2003) and **d** data for lattice thickness from Guidry and Grinnell (1985). In each case, the 'best-fit' values of $\bar{\theta}$ and $\bar{k}$ that yield the lowest χ^2 are indicated by a cross within a circle

where i correspond to all the experimental data points being considered, $\mathscr{E}_i$ are the values of $l(t)$ for these data points and $\mathscr{O}_i$ are the corresponding values of $1 + W(T)$ obtained from the simulations. As shown in Table 2, we find that the χ^2 values, obtained by using the optimal values of $\bar{\theta}$ and $\bar{k}$ for each case, are in the range 0.004–0.059, indicating a good fit between theory and experiments.

To test the robustness of these fits, we determine the values of χ^2 obtained by simulating our model for a wide range of choices of $\bar{\theta}$ and $\bar{k}$. In Fig. 6, we display contour plots that indicate how χ^2 varies with $\bar{\theta}$ and $\bar{k}$ for each of the four experiments mentioned earlier. In addition, for each case we display the location of the 'optimal' choice of $\bar{\theta}$ and $\bar{k}$, obtained through the minimisation procedure described
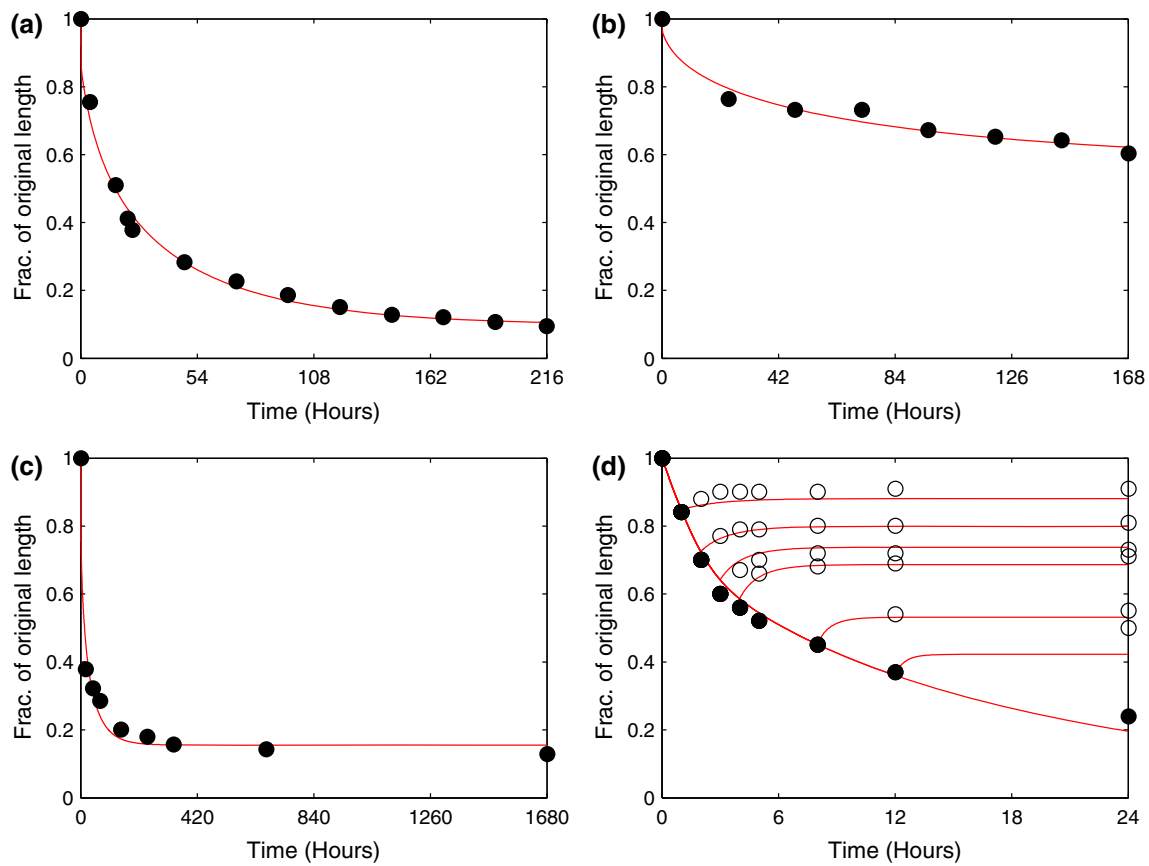
Fig. 7 Data for the fraction of the original length (diameter or thickness) of the FPCL, taken from different experiments (denoted by *dark circles*), superimposed with numerical results for $l(t)$ (from the expression (24), and denoted by *red solid lines*) obtained by simulating the system (22)–(23). The parameters $\bar{\mu}$, $\bar{\tau}$ and $\bar{e}_{\mathrm{crit}}$ are estimated heuristically from available information for each experiment, and the values used for simulations in each case are listed in Table 1. The corresponding best-fit values of $\bar{\theta}$ and $\bar{k}$ are listed in Table 2. Fits are shown for **a** data for lattice diameter from Bell et al. (1979), **b** data for lattice diam-

eter from Talas et al. (1997), **c** data for lattice diameter from Feng et al. (2003) and **d** data for lattice thickness from Guidry and Grinnell (1985). Experimental data are available for six different cases in (Guidry and Grinnell 1985), for which lattice reorganisation is inhibited through the addition of cytochalasin D at different times T_{inh}. We simulate this inhibition by setting $N(X, T) = 0$ at $T = T_{\mathrm{inh}}$, and the results are displayed for each corresponding case. Note that the model captures the partial re-expansion of the lattice (*empty circles*) observed in the experiment

above. It can be observed from this figure that small perturbations (around $\pm 10\%$) in the value of either of the two parameters from the global minima will not substantially change the resulting values of χ^2. Indeed, as seen in Table 2, the corresponding χ^2 values in these cases are of a similar order of magnitude to those obtained when using the best-fit values of $\bar{\theta}$ and $\bar{k}$. This implies that the global minima displayed in Fig. 6 can be used to obtain robust fits of the simulations to each of the four datasets.

It is important to note that our choice of the global minima of χ^2 is in order to provide a unifying criterion for the selection of $\bar{\theta}$ and $\bar{k}$. Although the best-fit values listed in Table 2 vary over a wide range, there is a large region of the $(\bar{\theta}, \bar{k})$-space over which we could obtain fits that are essentially as good (see Fig. 6). Thus, one could have, in principle, chosen very similar values of $\bar{\theta}$ and $\bar{k}$ for each of the three free-floating FPCL experiments and have still obtained good

fits in each case. While such a choice might potentially be more realistic, as one would not expect much variance of these parameters across different free-floating FPCLs, it is difficult to justify the use of any pair of $(\bar{\theta}, \bar{k})$ over another. To this end, we restrict our attention to the best-fit values in Table 2.

We next examine in detail the best fits to the individual datasets. The data for the change in the fraction of the original lattice extent for four different experiments are shown in Fig. 7. It is important to note from Table 1 that the lattices for the four chosen experiments have very different spatial extents, which explains the differing timescales for contraction. In fact, it appears that the rate at which the fraction of the original extent of a lattice shrinks is inversely proportional to its original extent. This suggests that the contraction rate of the lattices is related to their initial sizes.

We begin by considering the experiments performed by Bell et al. (1979) that yielded the first reported observation of FPCL contraction. In these experiments, different numbers of fibroblast cells were embedded in free-floating collagen lattices of varying ECM density, which contained foetal bovine serum. The fraction of the original length was then measured at various times over the course of several days. In the following, we consider their set of results that were obtained using 7.5×10^6 fibroblast cells embedded in a lattice of initial diameter 53 mm. It was observed that this lattice subsequently contracted to around 10% of its original diameter in around 9 days. We find that the best fit of our numerical results to the experimental data can be obtained by using $\bar{\theta} = 0.89$, $\bar{k} = 106.62$ (see Fig. 7a).

We next consider the experiments of Talas et al. (1997), in which the difference between the effects of normal and recessive dystrophic epidermolysis bullosa fibroblasts were investigated. For the case of normal fibroblasts, 2.5×10^5 cells were embedded in a lattice with a diameter of approximately 2.18 cm. It was observed that the lattice contracted to around 37% of its original area in around 7 days. We find that the best fit of our numerical results to the experimental data can be obtained by using $\bar{\theta} = 5.10$, $\bar{k} = 1294.92$ (see Fig. 7b).

Next, we consider the experiments of Feng et al. (2003), in which the mechanical properties of contracted collagen gels were investigated. Here, 2.5×10^6 fibroblast cells were embedded within a lattice of initial diameter 100 mm. It was observed that the lattice contracted to around 13% of its original diameter by the end of the experiment, with most of the contraction occurring within the first few days. In this case, we find that the best fit of our numerical results to the experimental data can be obtained by using $\bar{\theta} = 16.14$, $\bar{k} = 183.85$ (see Fig. 7c).

Finally, we consider the results of Guidry and Grinnell (1985), obtained when 10^5 fibroblasts were placed on an attached lattice of diameter 12 mm. It was observed that this lattice contracted to about 24% of its original thickness in around 1 day. As the presence of protomyofibroblasts was not reported in these experiments, it is likely that the observed contraction is primarily due to the activity of fibroblasts and hence our model can be used to approximate this behaviour. We simulate the effect of adding cytochalasin D by allowing $N(X, T)$ to take the form (20). Results obtained using $\bar{\theta} = 0.33$, $\bar{k} = 2.97$, which gave the best fit to the experimental data, are shown in Fig. 7d. We find that in addition to the contraction of this gel, our model can capture the observed partial re-expansion.

4 Discussion

In this work, we develop a 1-D morphoelastic model to describe the evolution of the diameter (width) of a free-floating (attached) collagen lattice that is contracted by fibroblasts. We fit numerical solutions of the model to previously obtained experimental data by optimising two free parameters. In addition to being able to capture the contraction of the lattice, our model closely describes the partial re-expansion of the lattice observed in the experiment by Guidry and Grinnell (1985). Hence, this is to our knowledge the first mathematical model that explains how the permanent contraction of such lattices partially persists when reorganisation is inhibited by killing the fibroblasts or by otherwise preventing them from altering the lattice. We achieve this by explicitly taking into account the continual changes to the zero stress state of a material in response to a prescribed rate of growth and explicitly describes the evolution of this state. The partial re-expansion of the lattice is an example of a class of phenomena related to changes in the underlying tissue structure. As the theoretical framework developed here is flexible and versatile, it could potentially be used to model a range of other biological processes that involve internal remodelling of a tissue's mechanical structure, by making certain assumptions about the dependence of growth on other physical parameters.

Note that our framework for stress and strain is developed in Eulerian coordinates (in 'Appendix 1'). Although a Lagrangian framework can lead to equations with fixed boundaries and a useful variational structure (see, for example Roberts (1994) and Gonzalez and Stuart (2008)), it is typically only appropriate in situations where the zero stress state does not evolve. However, as described in Yavari (2010), the introduction of a changing zero stress state leads to new terms that need to be carefully incorporated into the energy balance equation. Moreover, in cases where the zero stress state is close to the current state, but quite different from the initial state, Eulerian coordinates enable aspects of small deformation theory, such as the linear stress–strain relationship, to be applied.

On deriving the relations for stress and strain in Eulerian coordinates, we then revert to Lagrangian coordinates (in 3.2) in order to avoid the problems inherent in a system with a moving boundary. To do this, we exploit the fact that a conversion to Lagrangian coordinates corresponds to a conversion to characteristic variables (as diffusion is absent in our system), and we are thus able to simplify our model to a system of ordinary differential equations.

It should be noted that we have assumed in our model that the zero stress state is always uniform within each unit and that the expression for $g(x, t)$ also gives a uniform rate of change to the zero stress state. Against this, it might be argued that the only region where the zero stress state is changing (due to the direct effect of fibroblast action) is the region where $-l_c < x < l_c$. However, experiments have been performed where cells were cultured on top of lattices instead of throughout lattices, and these still showed relatively uniform

contraction (Grinnell and Lamke 1984; Guidry and Grinnell 1985, 1986). This indicates that while cell migration may be slow (Grinnell and Lamke 1984; Ascione et al. 2016), there is sufficient cell movement (or perhaps cells rearrange collagen over sufficiently large volumes) for it to be reasonable to assume that the change in the zero stress state is uniform in space.

Despite the fact that cell movement is quite limited over the time scale of FPCL contraction, a natural extension to our model would be to consider the case where cell density is non-uniform, and where there is active cell movement over the timescale of contraction. Extensions like this would be necessary for developing models of wound healing based on the principles presented in this model. When cell motility is taken into consideration, the transformation to Lagrangian coordinates would no longer convert the partial differential equations of the original model to ordinary differential equations, and it is likely that it would be more straightforward to solve the original Eulerian equations.

The morphoelastic approach detailed in this paper, where an evolution law is developed for the effective strain but a conventional stress–strain relationship is used, could potentially be applied to several other biological processes including soft tissue growth, arterial remodelling, aneurysm development, morphogenesis, initiation of stretch marks and solid tumour growth. Furthermore, the permanent contraction observed in some pathological scars instead suggests that morphoelastic changes to the underlying extracellular matrix are particularly significant during the wound healing process. Hence, an important potential application of this theory is the development of a mechanochemical model of dermal wound healing. Indeed, it would be fruitful to build on recent theoretical models of the wound healing process that have considered aspects of the interplay between fibroblasts, keratinocytes and growth factors (Menon et al. 2012), the complementary rôles of TGF-β and tissue tension (Murphy et al. 2011a, 2012), the interplay between these components and ECM deformation (Valero et al. 2014), and their rôle in hypertrophic scar formation (Koppenol et al. 2017b) and wound retraction (Koppenol et al. 2017a).

In addition, there are several possible ways in which this model could be extended to describe other observed aspects of the behaviour of FPCLs. For instance, there have been experiments in which force measurement devices were attached to the collagen lattice (Kolodney and Wysolmerski 1992; Brown et al. 1996; Marenzana et al. 2006) in order to measure the total contractile force exerted by the cells. In each case, the force measurement device provides a finite spring-like resistance to the contraction of the lattice, and so the contraction process could be described using our model by replacing the stress-free boundary condition in (13) with one that relates the stress at $x = l(t)$ to the displacement at the contracting edge. However, as the increased elastic ten-

sion in such a lattice could lead fibroblasts to modulate into protomyofibroblasts (Tomasek et al. 2002) that increase the stress, it may also be necessary to make the cell-associated stress, σ_c, a function of elastic stress. Indeed, this modulation can also occur in stress-relaxed FPCLs (Tomasek et al. 1992), which causes the lattice to contract rapidly when released. In the additional presence of TGF-β, protomyofibroblast cells in such lattices will further modulate into myofibroblasts (Desmoulière et al. 1993; Tomasek et al. 2002; Gabbiani 2003; Desmoulière et al. 2005). In order to capture the effect of these highly contractile cells, our model could be modified via the addition of a new species for protomyofibroblasts (or myofibroblasts), a new chemical species, TGF-β, and including a conversion term in the equation for the fibroblasts. Furthermore, as mentioned earlier, the effect of heterogeneity in gel compaction could also be investigated using the theoretical framework that we describe.

However, it is important to note that although our morphoelastic model closely captures the important features of the permanent contraction of FPCLs, the approach used here can only truly be justified in 1-D Cartesian coordinates (see Appendix section 'The multiplicative decomposition of the deformation gradient' for more details). Consequently, although our model can provide a good description of attached lattices, a complete description of cylindrical, free-floating lattices would require significant modifications to the constitutive laws used for the mechanics of the lattice (albeit with only minor adjustments to the reaction-diffusion equations). This could still be achieved using the same principles described in Sect. 3.1 if appropriate modifications are made; for example, we could consider a three-dimensional array of units, each containing a single cell, and each cell could be treated as a sphere of body stresses pulling inward. By homogenising such a system, we could develop a three-dimensional constitutive law for growth analogous to (7); however, any such rule would be significantly more complicated than the one-dimensional rule developed in this manuscript.

An additional complication in this regard is that there remains considerable ambiguity surrounding the precise specification of 3-D laws for the evolution of the zero stress state (for an overview on recent advances in this area, see Kuhl (2014)). As noted in Ambrosi et al. (2011), there has been little success in using thermodynamic arguments to develop general frameworks for morphoelasticity. Furthermore, there are uniqueness issues surrounding the multiplicative decomposition of the deformation gradient and it is difficult to ensure that any phenomenological evolution law is appropriately observer independent. Although some effort has gone into resolving these problems (especially in the engineering literature—see, for example, Lubarda (2001) and Xiao et al. (2006)), the resulting models are often densely expressed and difficult to apply to biological morphoelastic-

ity. As noted in Chaps. 4 and 5 of Hall (2008), some progress can be made by considering possible three-dimensional generalisations of (31), but there is a need for further work in this area. We also note that there is still interest in developing constitutive models that could provide better mathematical descriptions of remodelling in soft biological tissues (see, for example, Comellas et al. (2016)).

Despite these challenges, the morphoelastic framework presented in this manuscript has significant advantages over other approaches to describing biological remodelling. In particular, phenomena like the permanent contraction of a collagen lattice, which our model can describe, are inaccessible to classical Kelvin–Voigt models and are very different from the stress-induced contraction observed in Maxwell models.

The central achievement of our work lies in developing a theoretical framework for the mechanics of tissue remodelling that explicitly accounts for the action of cells to change the fundamental structure of a collagen lattice. By defining strain in terms of the difference between the current state and the zero stress state and considering how this strain changes according to both physical deformation and the action of cells, we find that morphoelasticity can be easily incorporated into a model of FPCL contraction. Indeed, this approach allows us to use conventional constitutive laws to relate the stress to the strain. The 1-D morphoelastic framework described in this paper provides us with a simple and meaningful technique to describe some of the complexities of biological remodelling, and it has the potential to be extended and used in a wide range of other areas.

Appendix 1: effective strain and contraction in a 1-D morphoelastic body

The multiplicative decomposition of the deformation gradient

The idea that an observed deformation gradient tensor F could be expressed in terms of elastic and plastic tensor fields through a multiplicative decomposition was first introduced by Bilby et al. (1957) and Kröner (1958, 1959). This was further developed by Stojanović et al. (1964, 1970) in the context of thermoelasticity and Lee (1969) for the description of metal plasticity at large deformations, while Rodriguez et al. (1994) and Cook (1995)

were the first to utilise this in the context of biomechanics. The pioneering work of Rodriguez et al. (1994) and Cook (1995) was later extended and expanded by Hoger and coworkers (see especially Chen and Hoger (2000)), Goriely and coworkers (Ben Amar and Goriely 2005; Goriely and Ben Amar 2007; Goriely et al. 2008), Ambrosi and coworkers (Ambrosi and Mollica 2004; Ambrosi and Guana 2007; Ambrosi and Guillou 2007) and by Vandiver (2009). This biological work has developed alongside applications to thermoelasticity and plasticity, and achievements in these areas have informed each other. This is exemplified by the cross-disciplinary work of Lubarda (2001, 2004) and Rajagopal and coworkers (see, for example, Rajagopal and Srinivasa (2004)). For a comprehensive review of the history and applications of the multiplicative decomposition of deformation gradient, see Lubarda (2004).

In a recent comprehensive review of current work on modelling growth and remodelling, Ambrosi et al. (2011) describe a number of applications of the multiplicative decomposition of the deformation gradient, ranging from the remodelling of heart muscle to morphogenesis. The multiplicative decomposition of the deformation gradient is now being used in models of biomechanical phenomena ranging from tissue growth (Ben Amar and Goriely 2005) to the operation of the heart (Göktepe and Kuhl 2010; Rausch et al. 2011), although it is important to note that this approach will only be valid when the tissue behaves elastically on the timescale of remodelling (Jones and Chapman 2012) and that some authors have general reservations about the use of the multiplicative decomposition on theoretical grounds (Xiao et al. 2006). Indeed, Ambrosi et al. (2011) note that there are problems and ambiguities to be resolved when developing appropriate laws to describe the evolution of the growth part of the deformation gradient in response to remodelling. In the context of the present work, it is important to note that many of these difficulties are avoided as we restrict our analysis to the one-dimensional (1-D) Cartesian case, although it is still necessary to ensure that the constitutive relation is appropriate for the type of remodelling under consideration.

An accessible introduction to the use of the multiplicative decomposition in biological applications can be found in Goriely and Moulton (2011), which begins with an analysis of a 1-D growing material that is relevant to the research presented here. It is important to note that a 1-D body can never be residually stressed: it is impossible to encounter the situation in which the zero stress state cannot be achieved without introducing cuts. Moreover, ensuring observer independence of time derivatives is much simpler along a single dimension, as it excludes the possibility of a rotating observer. We now develop a simple mathematical framework for modelling the growth or contraction of a 1-D Cartesian morphoelastic body.

Strain evolution

The deformation gradient is given by the scalar function

$$F(X, t) = \frac{\partial x}{\partial X},$$

Following the 1-D version of Eq. (1) in Goriely and Moulton (2011), we express this as the product

$$F = \alpha \gamma, \tag{29}$$

where the elastic stretch α is the local size ratio between the current state and the zero stress state, and the growth stretch γ is the local size ratio between the zero stress state and the initial state (the growth stretch).

In Goriely and Moulton (2011), the constitutive relation for 1-D growth is assumed to depend on the rate of growth $g(x, t)$:

$$\frac{\partial \gamma}{\partial t} = g(x, t), \tag{30}$$

While (30) is useful at small deformations (*i.e.* when $F \approx 1$), it leads to inconsistencies if the current state is significantly different from the initial state, as in the case of FPCL contraction. In order to obtain an equivalent of (30) for large deformations, we first note that $g(x, t)$ should satisfy

$$\frac{\mathrm{d}}{\mathrm{d}t} \int_{X_A}^{X_B} \gamma(X, t)\, \mathrm{d}X = \int_{x(X_A, t)}^{x(X_B, t)} g(x, t)\, \mathrm{d}x. \tag{31}$$

That is, $g(x, t)$ should be defined with reference to the current configuration, but it should measure the rate of change of the zero stress state of any collection of material particles. It follows from (31) that $g(x, t)$ is related to the material derivative of $\gamma(X, t)$:

$$\frac{\mathrm{D}\gamma}{\mathrm{D}t} = F g(x, t), \tag{32}$$

Note that this reduces to (30) when $F \equiv 1$.

Now, we expect that the stress at any point in the body will be related to the difference between the zero stress state and the current state. A plausible constitutive law that relates the stress, σ, to the elastic stretch, α is

$$\sigma = E\left(1 - \alpha^{-1}\right), \tag{33}$$

where E is the Young's modulus. This is analogous to Hooke's law for a linear elastic material, but uses an Eulerian rather than a pseudo-Lagrangian measure of strain, since

$$e^E \equiv 1 - \alpha^{-1} = \lim_{\Delta x \to 0} \frac{\Delta x - \Delta z}{\Delta x}, \text{ while}$$

$$e^L \equiv \alpha - 1 = \lim_{\Delta x \to 0} \frac{\Delta x - \Delta z}{\Delta z},$$

where Δx and Δz relate to the changes in the current and zero stress states, respectively. In cases where the current state is close to the zero stress state, and hence, $\alpha \approx 1$, we see that $e^E \approx e^L$ and (33) is equivalent to other plausible constitutive laws, such as those in Goriely and Moulton (2011):

$$\sigma = E(\alpha - 1), \tag{34}$$

$$\sigma = \frac{E}{3}\left(\alpha^2 - \alpha^{-1}\right), \tag{35}$$

Experimental observations indicate that most of the change in size of a contracting FPCL is due to the permanent rearrangement of fibres by fibroblasts (Guidry and Grinnell 1985). Hence, it is appropriate to use (33) and assume a linear relationship between stress and strain, rather than the nonlinear model (35). Moreover, (33) has an interesting advantage over (34) and (35), namely that the evolution of Eulerian strain in response to growth can neatly be expressed as an advection equation with a source term that is independent of e^E.

In order to see this, we substitute (29) into (32) to obtain

$$F \frac{\mathrm{D}}{\mathrm{D}t} \alpha^{-1} + \alpha^{-1} \frac{\mathrm{D}F}{\mathrm{D}t} = F g(x, t). \tag{36}$$

Since $F^{-1} \mathrm{D}F/\mathrm{D}t = \partial v/\partial x$ where v is the velocity and where $\partial v/\partial x$ is the velocity gradient, it follows that α^{-1} satisfies the equation

$$\frac{\partial}{\partial t} \alpha^{-1} + \frac{\partial}{\partial x}\left(v\, \alpha^{-1}\right) = g(x, t),$$

and using $e^E \equiv 1 - \alpha^{-1}$ we thus obtain the mechanical model for a morphoelastic solid with small effective strain

$$\frac{\partial e^E}{\partial t} + \frac{\partial}{\partial x}\left(e^E v\right) = \frac{\partial v}{\partial x} - g(x, t), \tag{37}$$

Note that thus far we have made the assumption that the relation between stress and strain is purely elastic

$$\sigma = E e^E.$$

However, as discussed in Sect. 3.1, this can easily be extended to viscoelastic bodies through the use of a Kelvin–Voigt viscoelastic constitutive law. In Sect. 3 of the main text, we use this formulation together with (37) to derive a set of governing equations for the contraction of a 1-D morphoelastic body.

Appendix 2: derivation of the spatial and temporal transformations between coordinate systems

In one spatial dimension, we use X to represent the Lagrangian coordinate and x to represent the Eulerian coordinate. At any given time t, there will be a one-to-one mapping from the initial configuration to the current configuration. Thus, we can always write $X = X(x, t)$ and $x = x(X, t)$; moreover, the fact that particles are not permitted to move through each other implies that $\partial x / \partial X > 0$.

Now, the Eulerian displacement gradient is the spatial derivative of $u(x, t) = x - X(x, t)$, i.e.

$$w(x, t) = 1 - \frac{\partial X}{\partial x}. \tag{38}$$

Similarly, the Lagrangian displacement gradient is

$$W(X, T) = \frac{\partial}{\partial X} (x - X) = \frac{1}{1 - w} - 1.$$

We thus have the relation

$$1 + W = \frac{1}{1 - w}. \tag{39}$$

Using the chain rule, the Eulerian spatial derivative is

$$\frac{\partial}{\partial x} \equiv \frac{\partial X}{\partial x} \frac{\partial}{\partial X} + \frac{\partial T}{\partial x} \frac{\partial}{\partial T}.$$

The derivative $\partial T / \partial x$ is equal to zero, and using (38) we obtain the expression

$$X = x - \int_0^x w(\xi, t) \mathrm{d}\xi. \tag{40}$$

Furthermore, using (38) and (39), we obtain the following transformation for the spatial derivative

$$\frac{\partial}{\partial x} \equiv \frac{1}{1 + W} \frac{\partial}{\partial X}. \tag{41}$$

We similarly use the chain rule to obtain the following expression for the Eulerian temporal derivative

$$\frac{\partial}{\partial t} \equiv \frac{\partial X}{\partial t} \frac{\partial}{\partial X} + \frac{\partial T}{\partial t} \frac{\partial}{\partial T}.$$

The derivative $\partial T / \partial t$ is equal to one, and so using (40) we have

$$\frac{\partial}{\partial t} \equiv \frac{\partial}{\partial t} \left(\int_0^x 1 - w(\xi, t) \, \mathrm{d}\xi \right) \frac{\partial}{\partial X} + \frac{\partial}{\partial T}.$$

Using (15), we have

$$\frac{\partial}{\partial t} \equiv \int_0^x \frac{\partial}{\partial \xi} (w(\xi, t) \, v(\xi, t) - v(\xi, t)) \, \mathrm{d}\xi \frac{\partial}{\partial X} + \frac{\partial}{\partial T},$$

which, on using (39) and the fact that $v(0, t) = 0$, yields

$$\frac{\partial}{\partial t} \equiv \frac{\partial}{\partial T} - \frac{v}{1 + W} \frac{\partial}{\partial X}.$$

Now, from (10), we have $v(1 - w) = \partial u / \partial t$. Since $u \equiv U$, using the above expression in conjunction with (39), this yields

$$v = (1 + W) \left(V - \frac{v}{1 + W} W \right),$$

where we have used the definitions of V and W. This implies that $v \equiv V$, and so we obtain the following transformation for the temporal derivative

$$\frac{\partial}{\partial t} \equiv \frac{\partial}{\partial T} - \frac{V}{1 + W} \frac{\partial}{\partial X}. \tag{42}$$

Now, from (15) we have $\partial w / \partial t + \partial (w \, v) / \partial x = \partial v / \partial x$. Using (39), (41) and (42), this reduces to the following relation between the Lagrangian displacement gradient and velocity:

$$\frac{\partial W}{\partial T} = \frac{\partial V}{\partial X}. \tag{43}$$

We use this expression in Sect. 3.2 of the main text to derive our morphoelastic model of FPCL contraction.

References

Amadeu TP, Coulomb B, Desmoulière A, Costa AMA (2003) Cutaneous wound healing: myofibroblastic differentiation and in vitro models. Int J Low Extrem Wounds 2(2):60–68. doi:10.1177/1534734603256155

Ambrosi D, Mollica F (2004) The role of stress in the growth of a multicell spheroid. J Math Biol 48(5):477–499. doi:10.1007/s00285-003-0238-2

Ambrosi D, Guana F (2007) Stress modulated growth. Math Mech Solids 12(3):319–343. doi:10.1177/1081286505059739

Ambrosi D, Guillou A (2007) Growth and dissipation in biological tissues. Continuum Mech Therm 19(5):245–251. doi:10.1007/s00161-007-0052-y

Ambrosi D, Ateshian GA, Arruda EM, Cowin SC, Dumais J, Goriely A, Holzapfel GA, Humphrey JD, Kemkemer R, Kuhl E, Olberding JE, Taber LA, Garikipati K (2011) Perspectives on biological growth and remodeling. J Mech Phys Solids 59(4):863–883. doi:10.1016/j.jmps.2010.12.011

Arora PD, Narani N, McCulloch CAG (1999) The compliance of collagen gels regulates transforming growth factor-β induction of α-smooth muscle actin in fibroblasts. Am J Pathol 154(3):871–882. doi:10.1016/S0002-9440(10)65334-5

Ascione F, Vasaturo A, Caserta S, D'Esposito V, Formisano P, Guido S (2016) Comparison between fibroblast wound healing and cell random migration assays in vitro. Exp Cell Res 347(1):123–132. doi:10.1016/j.yexcr.2016.07.015

Augusteyn RC (2010) On the growth and internal structure of the human lens. Exp Eye Res 90(6):643–654. doi:10.1016/j.exer.2010.01.013

Barocas VH, Tranquillo RT (1994) Biphasic theory and in vitro assays of cell-fibril mechanical interactions in tissue-equivalent collagen gels. In: Mow VC, Guilak F, Tran-Son-Tay R, Hochmuth RM (eds) Cell Mechanics and Cellular Engineering. Springer, Berlin, pp 185–209

Barocas VH, Tranquillo RT (1997) An anisotropic biphasic theory of tissue-equivalent mechanics: the interplay among cell traction, fibril alignment and cell contact guidance. J Biomech Eng 119:137–145. doi:10.1115/1.2796072

Barocas VH, Moon AG, Tranquillo RT (1995) The fibroblast-populated collagen microsphere assay of cell traction force—Part 2: measurement of the cell traction parameter. J Biomech Eng 117(2):161–170. doi:10.1115/1.2795998

Bell E, Ivarsson B, Merrill C (1979) Production of a tissue-like structure by contraction of collagen lattices by human fibroblasts of different proliferative potential in vitro. Proc Natl Acad Sci USA 76(3):1274–1278

Bellows CG, Melcher AH, Aubin JE (1981) Contraction and organization of collagen gels by cells cultured from periodontal ligament, gingiva and bone suggest functional differences between cell types. J Cell Sci 50(1):299–314

Bellows CG, Melcher AH, Bhargava U, Aubin JE (1982) Fibroblasts contracting three-dimensional collagen gels exhibit ultrastructure consistent with either contraction or protein secretion. J Ultrastruct Mol Struct Res 78(2):178–192. doi:10.1016/S0022-5320(82)80022-1

Ben Amar M, Goriely A (2005) Growth and instability in elastic tissues. J Mech Phys Solids 53(10):2284–2319. doi:10.1016/j.jmps.2005.04.008

Bilby BA, Gardner LRT, Stroh AN (1957) Continuous distributions of dislocations and the theory of plasticity. In: Proceedings of the 9th international congress of applied mechanics, vol 8. pp 35–44

Bowden LG, Byrne HM, Maini PK, Moulton DE (2016) A morphoelastic model for dermal wound closure. Biomech Model Mechanobiol 15(3):663–681. doi:10.1007/s10237-015-0716-7

Brown RA, Talas G, Porter RA, McGrouther DA, Eastwood M (1996) Balanced mechanical forces and microtubule contribution to fibroblast contraction. J Cell Physiol 169(3):439–447. doi:10.1002/(SICI)1097-4652(199612)169:3<439::AID-JCP4>3.0.CO;2-P

Carlson MA, Longaker MT (2004) The fibroblast-populated collagen matrix as a model of wound healing: a review of the evidence. Wound Repair Regen 12(2):134–147. doi:10.1111/j.1067-1927.2004.012208.x

Chandran PL, Barocas VH (2004) Microstructural mechanics of collagen gels in confined compression: poroelasticity, viscoelasticity, and collapse. J Biomech Eng 126(2):152–166. doi:10.1115/1.1688774

Chen YC, Hoger A (2000) Constitutive functions of elastic materials in finite growth and deformation. J Elasticity 59(1–3):175–193. doi:10.1023/A:1011061400438

Clement CF (1978) Solutions of the continuity equation. Proc Royal Soc Lond A Math Phys Eng Sci 364(1716):107–119. doi:10.1098/rspa.1978.0190

Comellas E, Gasser TC, Bellomo FJ, Oller S (2016) A homeostatic-driven turnover remodelling constitutive model for healing in soft tissues. J R Soc Interface 13(116):20151081. doi:10.1098/rsif.2015.1081

Cook J (1995) Mathematical models for dermal wound healing: Wound contraction and scar formation. PhD thesis, University of Washington

Dallon JC, Ehrlich HP (2008) A review of fibroblast-populated collagen lattices. Wound Repair Regen 16(4):472–479. doi:10.1111/j.1524-475X.2008.00392.x

Desmoulière A, Geinoz A, Gabbiani F, Gabbiani G (1993) Transforming growth factor-β1 induces α-smooth muscle actin expression in granulation tissue myofibroblasts and in quiescent and growing cultured fibroblasts. J Cell Biol 122(1):103–111. doi:10.1083/jcb.122.1.103

Desmoulière A, Chaponnier C, Gabbiani G (2005) Tissue repair, contraction, and the myofibroblast. Wound Repair Regen 13(1):7–12. doi:10.1111/j.1067-1927.2005.130102.x

Discher DE, Janmey P, Wang YL (2005) Tissue cells feel and respond to the stiffness of their substrate. Science 310(5751):1139–1143. doi:10.1126/science.1116995

Eastwood M, Porter R, Khan U, McGrouther G, Brown R (1996) Quantitative analysis of collagen gel contractile forces generated by dermal fibroblasts and the relationship to cell morphology. J Cell Physiol 166(1):33–42. doi:10.1002/(SICI)1097-4652(199601)166:1<33::AID-JCP4>3.0.CO;2-H

Ehrlich HP (2003) The fibroblast-populated collagen lattice: a model of fibroblast collagen interactions in repair. In: DiPietro LA, Burns AL (eds) Wound healing. Springer, Berlin, pp 277–291

Ehrlich HP, Rajaratnam JBM (1990) Cell locomotion forces versus cell contraction forces for collagen lattice contraction: an in vitro model of wound contraction. Tissue Cell 22(4):407–417. doi:10.1016/0040-8166(90)90070-P

Ehrlich HP, Moyer KE (2013) Cell-populated collagen lattice contraction model for the investigation of fibroblast collagen interactions. In: Gourdie RG, Myers TA (eds) Wound regeneration and repair: methods and protocols, methods in molecular biology, vol 1037. Springer, New York, pp 45–58. doi:10.1007/978-1-62703-505-7_3

Elsdale T, Bard J (1972) Collagen substrata for studies on cell behavior. J Cell Biol 54(3):626–637. doi:10.1083/jcb.54.3.626

Enoch S, Leaper DJ (2005) Basic science of wound healing. Surgery 23(2):37–42. doi:10.1016/j.mpsur.2007.11.005

Evans MC, Barocas VH (2009) The modulus of fibroblast-populated collagen gels is not determined by final collagen and cell concentration: experiments and an inclusion-based model. J Biomech Eng 131(10):101014

Farsi JMA, Aubin JE (1984) Microfilament rearrangements during fibroblast-induced contraction of three-dimensional hydrated collagen gels. Cell Motil Cytoskel 4(1):29–40. doi:10.1002/cm.970040105

Feng Z, Yamato M, Akutsu T, Nakamura T, Okano T, Umezu M (2003) Investigation on the mechanical properties of contracted collagen gels as a scaffold for tissue engineering. Artif Organs 27(1):84–91. doi:10.1046/j.1525-1594.2003.07187.x

Ferrenq I, Tranqui L, Vailhé B, Gumery PY, Tracqui P (1997) Modelling biological gel contraction by cells: mechanocellular formulation and cell traction force quantification. Acta Biotheor 45(3–4):267–293. doi:10.1023/A:1000684025534

Fluck J, Querfeld C, Cremer A, Niland S, Krieg T, Sollberg S (1998) Normal human primary fibroblasts undergo apoptosis in three-dimensional contractile collagen gels. J Invest Dermatol 110(2):153–157. doi:10.1046/j.1523-1747.1998.00095.x

Fung YC (1993) Biomechanics: mechanical properties of living tissues. Springer, New York

Gabbiani G (2003) The myofibroblast in wound healing and fibrocontractive diseases. J Pathol 200(4):500–503. doi:10.1002/path.1427

Gabbiani G, Hirschel BJ, Ryan GB, Statkov PR, Majno G (1972) Granulation tissue as a contractile organ: a study of structure and function. J Exp Med 135(4):719–734. doi:10.1084/jem.135.4.719

García-Grajales JA, Jérusalem A, Goriely A (2016) Continuum mechanical modeling of axonal growth. Comput Methods Appl Mech Eng. doi:10.1016/j.cma.2016.07.032

Göktepe S, Kuhl E (2010) Electromechanics of the heart: a unified approach to the strongly coupled excitation–contraction problem. Comput Mech 45(2–3):227–243. doi:10.1007/s00466-009-0434-z

Gonzalez O, Stuart AM (2008) A first course in continuum mechanics. Cambridge University Press, Cambridge

Goriely A, Ben Amar M (2007) On the definition and modeling of incremental, cumulative, and continuous growth laws in morphoelasticity. Biomech Model Mechanobiol 6(5):289–296. doi:10.1007/s10237-006-0065-7

Goriely A, Moulton DE (2011) Morphoelasticity–a theory of elastic growth. In: Ben Amar M, Goriely A, Müller MM, Cugliandolo L (eds) New trends in the physics and mechanics of biological systems. Oxford University Press, Oxford

Goriely A, Robertson-Tessi M, Tabor M, Vandiver R (2008) Elastic growth models. In: Mondaini R, Pardalos PM (eds) Mathematical modelling of biosystems. Springer, Berlin, pp 1–45

Green JEF, Bassom AP, Friedman A (2013) A mathematical model for cell-induced gel compaction in vitro. Math Models Methods Appl Sci 23(1):127–163. doi:10.1142/S0218202512500479

Grinnell F (1994) Fibroblasts, myofibroblasts, and wound contraction. J Cell Biol 124(4):401–404. doi:10.1083/jcb.124.4.401

Grinnell F (2000) Fibroblast-collagen-matrix contraction: growth-factor signalling and mechanical loading. Trends Cell Biol 10(9):362–365. doi:10.1016/S0962-8924(00)01802-X

Grinnell F (2003) Fibroblast biology in three-dimensional collagen matrices. Trends Cell Biol 13(5):264–269. doi:10.1016/S0962-8924(03)00057-6

Grinnell F, Lamke C (1984) Reorganization of hydrated collagen lattices by human skin fibroblasts. J Cell Sci 66(1):51–63

Grinnell F, Ho CH, Lin YC, Skuta G (1999) Differences in the regulation of fibroblast contraction of floating versus stressed collagen matrices. J Biol Chem 274(2):918–923. doi:10.1074/jbc.274.2.918

Grinnell F, Ho CH, Tamariz E, Lee DJ, Skuta G (2003) Dendritic fibroblasts in three-dimensional collagen matrices. Mol Biol Cell 14(2):384–395. doi:10.1091/mbc.E02-08-0493

Guidry C, Grinnell F (1985) Studies on the mechanism of hydrated collagen gel reorganization by human skin fibroblasts. J Cell Sci 79(1):67–81

Guidry C, Grinnell F (1986) Contraction of hydrated collagen gels by fibroblasts: evidence for two mechanisms by which collagen fibrils are stabilized. Coll Relat Res 6(6):515–529

Hall CL (2008) Modelling of some biological materials using continuum mechanics. PhD thesis, Queensland University of Technology

Halliday NL, Tomasek JJ (1995) Mechanical properties of the extracellular matrix influence fibronectin fibril assembly in vitro. Exp Cell Res 217(1):109–117. doi:10.1006/excr.1995.1069

Harris AK, Wild P, Stopak D (1980) Silicone rubber substrata: a new wrinkle in the study of cell locomotion. Science 208(4440):177–179. doi:10.1126/science.6987736

Hinz B, Mastrangelo D, Iselin C, Chaponnier C, Gabbiani G (2001) Mechanical tension controls granulation tissue contractile activity and myofibroblast differentiation. Am J Pathol 159(3):1009–1020. doi:10.1016/S0002-9440(10)61776-2

Humphrey JD (2003) Continuum biomechanics of soft biological tissues. Proc Royal Soc Lond A Math Phys Sci 459(2029):3–46. doi:10.1098/rspa.2002.1060

Jones GW, Chapman SJ (2012) Modeling growth in biological materials. SIAM Rev 54(1):52–118. doi:10.1137/080731785

Kelynack KJ (2009) Cell-populated floating collagen lattices: an in vitro model of parenchymal contraction. In: Hewitson TD, Becker GJ (eds) Kidney research. Springer, Berlin, pp 1–11

Knapp DM, Barocas VH, Moon AG, Yoo K, Petzold LR, Tranquillo RT (1997) Rheology of reconstituted type I collagen gel in confined compression. J Rheol 41(5):971–993. doi:10.1122/1.550817

Knapp DM, Tower TT, Tranquillo RT, Barocas VH (1999) Estimation of cell traction and migration in an isometric cell traction assay. AIChE J 45(12):2628–2640. doi:10.1002/aic.690451219

Kolodney MS, Wysolmerski RB (1992) Isometric contraction by fibroblasts and endothelial cells in tissue culture: a quantitative study. J Cell Biol 117(1):73–82. doi:10.1083/jcb.117.1.73

Koppenol DC, Vermolen FJ, Niessen FB, Zuijlen PP, Vuik K (2017a) A biomechanical mathematical model for the collagen bundle distribution-dependent contraction and subsequent retraction of healing dermal wounds. Biomech Model Mechanobiol 16:345–361. doi:10.1007/s10237-016-0821-2

Koppenol DC, Vermolen FJ, Niessen FB, Zuijlen PP, Vuik K (2017b) A mathematical model for the simulation of the formation and the subsequent regression of hypertrophic scar tissue after dermal wounding. Biomech Model Mechanobiol 16:15–32. doi:10.1007/s10237-016-0799-9

Kröner E (1958) Kontinuumstheorie der versetzungen und eigenspannungen. Erg Angew Math 5:1–179

Kröner E (1959) Allgemeine kontinuumstheorie der versetzungen und eigensspannungen. Arch Ration Mech Anal 4(1):273–334

Kuhl E (2014) Growing matter: a review of growth in living systems. J Mech Behavior Biomed Mater 29:529–543. doi:10.1016/j.jmbbm.2013.10.009

Lee EH (1969) Elastic–plastic deformation at finite strains. J Appl Mech 36:1–6. doi:10.1115/1.3564580

Lin YC, Ho CH, Grinnell F (1997) Fibroblasts contracting collagen matrices form transient plasma membrane passages through which the cells take up fluorescein isothiocyanate-dextran and Ca^{2+}. Mol Biol Cell 8(1):59–71

Lubarda VA (2001) Elastoplasticity theory. CRC Press, Boca Raton

Lubarda VA (2004) Constitutive theories based on the multiplicative decomposition of deformation gradient: Thermoelasticity, elastoplasticity, and biomechanics. Appl Mech Rev 57(2):95–109. doi:10.1115/1.1591000

Majno G, Joris I (2004) Cells, tissues and disease: principles of general pathology, 2nd edn. Oxford University Press, New York

Marenzana M, Wilson-Jones N, Mudera V, Brown RA (2006) The origins and regulation of tissue tension: identification of collagen tension–fixation process in vitro. Exp Cell Res 312(4):423–433. doi:10.1016/j.yexcr.2005.11.005

Marquez JP, Genin GM, Zahalak GI, Elson EL (2005) The relationship between cell and tissue strain in three-dimensional bio-artificial tissues. Biophys J 88(2):778–789. doi:10.1529/biophysj.104.041947

Menon SN, Flegg JA, McCue SW, Schugart RC, Dawson RA, McElwain DLS (2012) Modelling the interaction of keratinocytes and fibroblasts during normal and abnormal wound healing processes. Proc Royal Soc Lond B Biol Sci 279(1741):3329–3338. doi:10.1098/rspb.2012.0319

Mochitate K, Pawelek P, Grinnell F (1991) Stress relaxation of contracted collagen gels: disruption of actin filament bundles, release of cell surface fibronectin, and down-regulation of DNA and protein synthesis. Exp Cell Res 193(1):198–207. doi:10.1016/0014-4827(91)90556-A

Moon AG, Tranquillo RT (1993) Fibroblast-populated collagen microsphere assay of cell traction force: Part 1. Continuum model. AIChE J 39(1):163–177. doi:10.1002/aic.690390116

Mudera VCi, (2000) Molecular responses of human dermal fibroblasts to dual cues: contact guidance and mechanical load. Cell Motil Cytoskel 45(1):1–9. doi:10.1002/(SICI)1097-0169(200001)45:1<1::AID-CM1>3.0.CO;2-J

Murphy KE, Hall CL, McCue SW, McElwain DLS (2011a) A two-compartment mechanochemical model of the roles of transforming

growth factor β and tissue tension in dermal wound healing. J Theor Biol 272(1):145–159. doi:10.1016/j.jtbi.2010.12.011

Murphy KE, McCue SW, McElwain DLS (2011b) Clinical strategies for contractures from a predictive mathematical model of dermal repair. Wound Rep Regen 20(2):104–202. doi:10.1111/j.1524-475X.2012.00775.x

Murphy KE, Hall CL, Maini PK, McCue SW, McElwain DLS (2012) A fibrocontractive mechanochemical model of dermal wound closure incorporating realistic growth factor kinetics. Bull Math Biol 74(5):1143–1170. doi:10.1007/s11538-011-9712-y

Murray JD (2001) Mathematical biology. II spatial models and biomedical applications. In: Interdisciplinary applied mathematics, vol 18. Springer, New York Incorporated

Patwari P, Lee RT (2008) Mechanical control of tissue morphogenesis. Circ Res 103(3):234–243. doi:10.1161/CIRCRESAHA.108.175331

Pryse KM, Nekouzadeh A, Genin GM, Elson EL, Zahalak GI (2003) Incremental mechanics of collagen gels: new experiments and a new viscoelastic model. Ann Biomed Eng 31:1287–1296. doi:10.1114/1.1615571

Rajagopal KR, Srinivasa AR (2004) On the thermomechanics of materials that have multiple natural configurations Part I: viscoelasticity and classical plasticity. Z Angew Math Physik 55(5):861–893. doi:10.1007/s00033-004-4019-6

Ramtani S (2004) Mechanical modelling of cell/ecm and cell/cell interactions during the contraction of a fibroblast-populated collagen microsphere: theory and model simulation. J Biomech 37(11):1709–1718. doi:10.1016/j.jbiomech.2004.01.028

Ramtani S, Fernandes-Morin E, Geiger D (2002) Remodeled-matrix contraction by fibroblasts: numerical investigations. Comput Biol Med 32(4):283–296. doi:10.1016/S0010-4825(02)00018-5

Rausch MK, Dam A, Göktepe S, Abilez OJ, Kuhl E (2011) Computational modeling of growth: systemic and pulmonary hypertension in the heart. Biomech Model Mechanobiol 10(6):799–811. doi:10.1007/s10237-010-0275-x

Rhee S, Grinnell F (2007) Fibroblast mechanics in 3D collagen matrices. Adv Drug Delivery Rev 59(13):1299–1305. doi:10.1016/j.addr.2007.08.006

Roberts AJ (1994) A one-dimensional introduction to continuum mechanics. World Scientific, Singapore

Rodriguez EK, Hoger A, McCulloch AD (1994) Stress-dependent finite growth in soft elastic tissues. J Biomech 27(4):455–467. doi:10.1016/0021-9290(94)90021-3

Roseborough IE, Grevious MA, Lee RC (2004) Prevention and treatment of excessive dermal scarring. J Natl Med Assoc 96(1):108–116

Rosenfeldt H, Grinnell F (2000) Fibroblast quiescence and the disruption of ERK signaling in mechanically unloaded collagen matrices. J Biol Chem 275(5):3088–3092. doi:10.1074/jbc.275.5.3088

Roy P, Petroll WM, Cavanagh HD, Chuong CJ, Jester JV (1997) An in vitro force measurement assay to study the early mechanical interaction between corneal fibroblasts and collagen matrix. Exp Cell Res 232(1):106–117. doi:10.1006/excr.1997.3511

Roy P, Petroll WM, Chuong CJ, Cavanagh HD, Jester JV (1999) Effect of cell migration on the maintenance of tension on a collagen matrix. Ann Biomed Eng 27(6):721–730. doi:10.1114/1.227

Sander LM (2013) Alignment localization in nonlinear biological media. J Biomech Eng 135(7):071006

Schreiber DI, Enever PAJ, Tranquillo RT (2001) Effects of PDGF-BB on rat dermal fibroblast behavior in mechanically stressed and unstressed collagen and fibrin gels. Exp Cell Res 266(1):155–166. doi:10.1006/excr.2001.5208

Schreiber DI, Barocas VH, Tranquillo RT (2003) Temporal variations in cell migration and traction during fibroblast-mediated gel compaction. Biophys J 84(6):4102–4114. doi:10.1016/S0006-3495(03)75135-2

Steinberg BM, Smith K, Colozzo M, Pollack R (1980) Establishment and transformation diminish the ability of fibroblasts to contract a native collagen gel. J Cell Biol 87(1):304–308. doi:10.1083/jcb.87.1.304

Stevenson MD, Sieminski AL, McLeod CM, Byfield FJ, Barocas VH, Gooch KJ (2010) Pericellular conditions regulate extent of cell-mediated compaction of collagen gels. Biophys J 99(1):19–28

Stojanović R, Djurić S, Vujošević L (1964) On finite thermal deformations. Arch Mech Stosow 16:103–108

Stojanović R, Vujošević L, Blagojević D (1970) Couple stresses in thermoelasticity. Rev Roum Sci Techn-Meć Appl 15:517–537

Stopak D, Harris AK (1982) Connective tissue morphogenesis by fibroblast traction: I. Tissue culture observations. Dev Biol 90(2):383–398. doi:10.1016/0012-1606(82)90388-8

Taber LA (1995) Biomechanics of growth, remodeling, and morphogenesis. Appl Mech Rev 48(8):487–545. doi:10.1115/1.3005109

Talas G, Adams TST, Eastwood M, Rubio G, Brown RA (1997) Phenytoin reduces the contraction of recessive dystrophic epidermolysis bullosa fibroblast populated collagen gels. Int J Biochem Cell B 29(1):261–270. doi:10.1016/S1357-2725(96)00132-X

Tamariz E, Grinnell F (2002) Modulation of fibroblast morphology and adhesion during collagen matrix remodeling. Mol Biol Cell 13(11):3915–3929. doi:10.1091/mbc.E02050291

Tomasek JJ, Haaksma CJ, Eddy RJ, Vaughan MB (1992) Fibroblast contraction occurs on release of tension in attached collagen lattices: dependency on an organized actin cytoskeleton and serum. Anat Rec 232(3):359–368. doi:10.1002/ar.1092320305

Tomasek JJ, Gabbiani G, Hinz B, Chaponnier C, Brown RA (2002) Myofibroblasts and mechano-regulation of connective tissue remodelling. Nat Rev Mol Cell Bio 3(5):349–363. doi:10.1038/nrm809

Tracqui P, Woodward DE, Cruywagen GC, Cook J, Murray JD (1995) A mechanical model for fibroblast-driven wound healing. J Biol Syst 3(4):1075–1084. doi:10.1142/S0218339095000976

Tranquillo RT, Murray JD (1992) Continuum model of fibroblast-driven wound contraction: inflammation-mediation. J Theor Biol 158(2):135–172. doi:10.1016/S0022-5193(05)80715-5

Valero C, Javierre E, García-Aznar JM, Gómez-Benito MJ (2014) A cell-regulatory mechanism involving feedback between contraction and tissue formation guides wound healing progression. PloS ONE 9(3):e92774. doi:10.1371/journal.pone.0092774

Vandiver R (2009) Morphoelasticity: the mechanics and mathematics of elastic growth. PhD Thesis, University of Arizona

Vandiver R, Goriely A (2009) Differential growth and residual stress in cylindrical elastic structures. Philos Trans Royal Soc Lond A Math Phys Eng Sci 367(1902):3607–3630. doi:10.1098/rsta.2009.0114

Vaughan MB, Howard EW, Tomasek JJ (2000) Transforming growth factor-β1 promotes the morphological and functional differentiation of the myofibroblast. Exp Cell Res 257(1):180–189. doi:10.1006/excr.2000.4869

Wakatsuki T, Kolodney MS, Zahalak GI, Elson EL (2000) Cell mechanics studied by a reconstituted model tissue. Biophys J 79(5):2353–2368. doi:10.1016/S0006-3495(00)76481-2

Xiao H, Bruhns OT, Meyers A (2006) Elastoplasticity beyond small deformations. Acta Mech 182(1–2):31–111. doi:10.1007/s00707-005-0282-7

Yang L, Witten TM, Pidaparti RM (2013) A biomechanical model of wound contraction and scar formation. J Theor Biol 332:228–48. doi:10.1016/j.jtbi.2013.03.013

Yavari A (2010) A geometric theory of growth mechanics. J Nonlinear Sci 20:781–830. doi:10.1007/s00332-010-9073-y

Zahalak GI, Wagenseil JE, Wakatsuki T, Elson EL (2000) A cell-based constitutive relation for bio-artificial tissues. Biophys J 79(5):2369–2381. doi:10.1016/S0006-3495(00)76482-4